
Chapter 2

FREQUENCY MEASUREMENT

2.0 Introduction

Frequency measurement is an important issue in Electrical engineering. Electric power systems have become increasingly complex over the last decade. The use of distributed generation, connection of non-linear loads and presence of unexpected system faults are the main causes of frequency variations. Power quality parameter includes frequency as an important index for measurement of power system stability.

In power system protection and control schemes it is necessary to accurately measure and track the fundamental power frequency under sinusoidal and non-sinusoidal conditions. The frequency deviation is a good indicator of the system abnormal operating conditions. Measurement of frequency is fast and accurate if the signal is purely sinusoidal. However, in reality the measured signals are distorted by higher harmonics and have time varying parameters. Since power electronics technology is increasingly applied in the power systems, it is required to detect frequency more precisely and faster in the presence of harmonics and noise. So many estimation methods have been developed offering different approaches to the problem such as zero crossing methods, FFT leakage [7], stationary phasor phase changes [8],

Kalman filtering [9] and least squares fitting [9]. The speed and accuracy of frequency measurement varies in each method. It is likely that method giving fast and accurate frequency measurement under non-sinusoidal conditions will be of great benefit to the utility.

Earlier day's determination of accurate frequency in power networks has become more complex. Few reasons are, dynamic balance between load and generation is a prerequisite for stable power system operation, which is more difficult to maintain due to expansion of transmission network which does not follow the growth of the system. The direct consequence is that the securities margins are generally smaller and quite often power systems operate at the brink of instability, possibly resulting in a blackout. Such operating practices imposed by the practical reasons are further exgravated due to the effects of deregulation. Non-utility generation and wheeling may reduce the stability margins of a normally secure system. It is therefore very important for utilities to develop measures monitor and control the dynamics of power system.

In distribution systems, a precise frequency measurement is necessary for frequency-protection relays. The required accuracy in the range of 5-10 mHz, and a very short frequency calculation time is also desirable. By connecting frequency relays at different locations with different settings, a controlled load-shedding and load-restoring program can be implemented

Fast and accurate frequency estimation in presence of noise attained a lot of attention as it is a challenging problem. Many solutions have been suggested, both in signal processing and in power system publications.

The classification is useful since different time demands put restrictions on what type of frequency estimator and filter technique can be used. In off-line data analysis we have access to the full time series and the estimation and filtering can be improved by using non-causal forward-backward filtering.

To compare different methods we need test criteria that reflect relevant demands. Three such demands are: speed of convergence; accuracy; and noise rejection. The key problem is to find a method that improves all these demand factors and not just compromise one demand for another.

2.1 Applications of Frequency Measurement

The typical use of frequency estimation in power systems is for protection scheme against loss of synchronism [10], under-frequency relaying and for power system stabilization [8]. Frequency estimation in power system has evolved along several paths.

➤ **Generator Protection:**

It is desired to have generator protection devices online during the start-up of generator. Especially it is important while operating the generator at low frequency. If the generator is started with a variable frequency drive (VFD), ground fault protection of the VFD is also desired by many utilities. Other protection functions such as over current protection should be active to detect short circuits after maintenance down time.

➤ **Feeder Protection, Load Shedding**

In distribution systems, a precise frequency measurement is necessary for frequency-protection relays. The required accuracy is in the range of 5-10 mHz, and a very short frequency calculation time is also desired. By connecting frequency relays at different locations with different settings, a controlled load-shedding and load restoring program can be implemented.

➤ **EHV Line Schemes, Synchronism Check**

For manual closing of the breaker, or for automatic reclosing after a three-pole trip with a long dead time, a precise calculation of the Bus and Line voltage is necessary. A reclosing is allowed, if the difference of voltage

amplitudes, phase angle between voltages, and frequency difference of these voltages are within acceptable limits. In a few networks having very long lines or stability problems, the ability to record the frequency deviation over time is useful.

2.2 Various Frequency Tracking Methods

2.2.1 Zero Crossing Methods

This is one of the popular methods for control applications. When using zero crossing methods, one determines the time difference between zero crossings of the signal to determine the frequency. This can be carried out by having a sliding window of N samples and curve fitting using a least squares technique [7]. This method can be applied to a single phase, but three phases may be used together to provide the frequency at more intervals. This method is not advisable in case of multiple zero crossings and under noisy conditions being present in the signal.

2.2.2 Quadratic Form

This method is described in detail in Hacaoglu [9]. Suppose that we are analyzing a set of signal samples defined by the vector $x = (x[n], x[n - 1], \dots, x[n - M + 1])^T$. The quadratic form of x is defined in Eq. 2.1

$$F(x) = \sum_{m=0}^{M-1} \sum_{k=0}^{M-1} h[k, m] x[n - k] x[n - m] \quad (2.1)$$

Where $h[k, m]$ is (k, m) the term of a $(M \times M)$ matrix, H , n is the number of sample, M is the total number of samples. T is the total sampling period. A nominal frequency of 50 Hz is assumed. In [7] it is shown that, by taking the ratio of two quadratic forms of x with different matrices H_1 and H_2 , it is possible to obtain an approximate formula for the frequency.

2.2.3 Discrete Fourier Transform With Phase Compensation

In this method, a DFT is computed over a 0.02 second segment of single-phase data and the phase at 50Hz is determined. By differentiation of this phase with respect to time, the frequency can be determined. In [7], this is extended to three phase data where the positive sequence DFT is used to compute the frequency. Since a minimum one cycle is required in DFT to compute the frequency DFT is computed over a period of 0.02 second.

2.2.4 Demodulation

Akke [8] suggested that if all the three phases of the signal are available, then one can form two signals $V_\alpha[n]$ and $V_\beta[n]$ that are 90° out of phase by application of α - β Transform. The complex signal is given by Eq. 2.2.

$$V[n] = V_\alpha[n] + jV_\beta[n] = Ae^{j(\omega_1 t_n + \Phi)} \quad (2.2)$$

Where ω_1 is the angular frequency at the n^{th} sample point, t_n is the corresponding period of sampling and Φ is the angle between the real and the imaginary part. In order to determine the frequency ω_1 , one demodulates $V[n]$ which may contain single frequency or multiple frequencies with the local oscillator term at angular frequency ω_0 . The unknown frequency of the signal is estimated as:

$$f[n] = f_0 + \frac{f_s}{2\pi} [\gamma[n] - \gamma[n-1]] \quad (2.3)$$

Where f_0 is the nominal frequency, f_s is the sampling frequency and γ is the phase difference between two consecutive samples.

2.2.5 Decomposition of Single Phase Into Orthogonal Components

In the (DSPOC) method of Moore [8], [9], which has been derived to analyze single phase data, the signal $s(t)$ is decomposed into two orthogonal components $x_1[t]$ and $x_2[t]$ by Eq. 2.4 and Eq. 2.5:

$$x_1(t) = \int_{-1/2T}^{1/2T} s(t - t') \sin(2\pi f_0 t') dt' \quad (2.4)$$

$$x_2(t) = \int_{-1/2T}^{1/2T} s(t - t') \cos(2\pi f_0 t') dt' \quad (2.5)$$

Where $T = 0.02s$ and f_0 is the reference frequency is taken to be 50 Hz.

Each filter represents a band pass filter centered at 50 Hz, but which have phase responses that are $\pi/2$ out of phase.

The frequency is estimated from Eq. 2.6:

$$f_e(t) = \frac{1}{2} \frac{[x_2(t)\dot{x}_1(t) - x_1(t)\dot{x}_2(t)]}{[x_1^2(t) + x_2^2(t)]} \quad (2.6)$$

Problem with this method is the gain of sine and cosine filters used in [8] are different from the reference frequency of 50 Hz. This can be overcome by using an adaptive normalization procedure [10]. The gains at present estimated frequency are computed for sine and cosine filters and this is used to renormalize the outputs x_1 and x_2 .

2.2.6 Non-Linear Least Squares Estimation

Various authors have approached the problem of determining the frequency deviation from mains using estimation techniques. The signal is modeled by Eq. 2.7

$$s(t) = A\cos(2\pi f_0 t + \phi_1(t)) \quad (2.7)$$

This can be rewritten as:

$$s(t) = x_1 \cos(2\pi(f_0 + f_1)t) - x_2 \sin(2\pi(f_0 + f_1)t) \quad (2.8)$$

Where

- x_1 Is in-phase component,
- x_2 Is quadrature phase component,
- f_0 Is reference frequency (50 Hz) and
- f_1 Is frequency deviation.

Girgis et al. [9] attempt a direct estimation of f_1 using Kalman filter techniques. The estimation problem in this technique is nonlinearity, $s(t)$ in (5) is a nonlinear function of x_1 , x_2 and f_1 , hence the Extended Kalman Filter needs to be used.

Recursive Least Squares (RLS) methods are applied to determine $\phi_1(t)$ which is numerically differentiated and smoothed to estimate the frequency deviation from f_0 . The filters used in this technique were quite complex.

2.2.7 Linear Estimation of Phase (LEP)

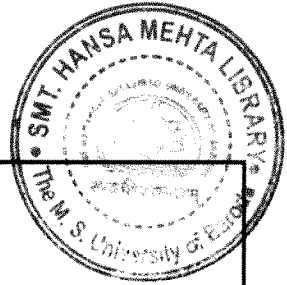
A novel approach [8], [9] follows on from algorithm of Kalman mentioned above but simplifies it to a linear estimation method to give amplitude and phase. Once phase angle is known then the frequency can be estimated, as it can be shown that the frequency error Δf is given by the time derivative of phase

Among the first technique of frequency measurement, those are based on zero crossing. They were gradually abandoned due to their sensitivity to noise, presence of DC components in the signal, and harmonics. However, their inherent simplicity cannot be matched by any other technique, this technique when combined with a data smoothing technique, may produce surprisingly good performance. A variation of the same method involves frequency multiplication of measured signal using PLL, which reduces the measurement time, but does not have very good resolution or dynamic properties. Phadke et al. [12] propose the Discrete Fourier Transform of the voltage samples to be used recursively for calculation of a stationary phasor, and positive sequence phasor rotation to be used for measurement of the frequency. The algorithm is inherently insensitive to harmonics because of the application of the DFT, but as proposed in [12], it is vulnerable to noise, and requires long measurement windows when frequency deviation from nominal is small.

All the methods have compromise between estimation of speed and accuracy. Some basic and well-known methods of frequency estimation are described in [11] while other new approaches are presented and analyzed in [7-12]. All the frequency detection methods work well under sinusoidal conditions. These methods are subjected to error in case of multiple zero crossings and non-sinusoidal conditions.

2.3 Digital Filters:

Since a digital filter is actually done by software which consists of calculations with data value, the component variations with analog filters are not present.



Advantages of digital filters are:

- High accuracy and performance.
- Linear phase and constant group delay (in FIR filters).
- No component drift problem.

. A general filter equation is given by Eq. 2.10.

$$\{x(i) = \text{input}; y(i) = \text{output at sampling time } i\} \tag{2.9}$$

$a(k)$ represents filter coefficients

$$y(n) = \sum_{j=0}^{N-1} x(n-j) - \sum_{k=1}^M a(k)(n-k) \tag{2.10}$$

The first term on right hand side is feed forward term and second is feedback term. If there is no second term present, then filter has only a **finite impulse response (FIR filter)**. With both terms present, it is an **infinite impulse response filter (IIR filter)**. As shown in Fig. 2.3-1 the block diagram of a typical FIR filter

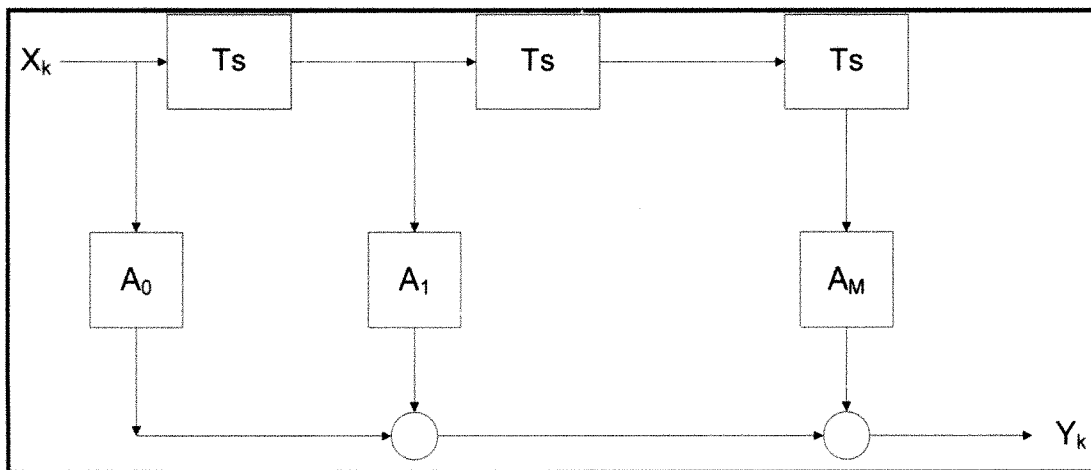


Fig. 2.3-1 Block diagram of a Digital FIR filter

2.4 Block Diagram of the Proposed System:

The proposed algorithm is modified version of Sezi's method [12]. This algorithm uses phase angle and amplitude information in order to compute frequency. The main advantage of this method is that it avoids waiting between zero crossings of the input signal.

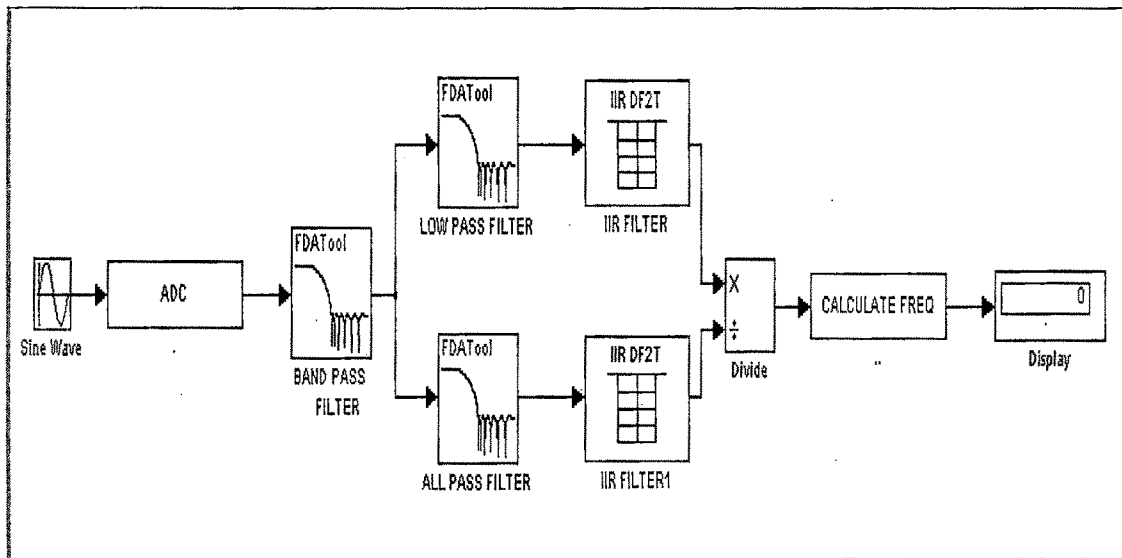


Fig. 2.4-1 Block diagram of frequency measurement for single-phase system.

As shown in the Fig. 2.4-1 the block diagram for measurement of the frequency using digital filters. The input signal used for measurement of frequency is a single phase voltage signal. Since a voltage signal is available anytime irrespective of the load therefore a voltage signal is used in the model. The time needed to reach the steady state is over three cycles but can be reduced if filter with shorter order are used.

The digital filters are initially designed and simulated on MATLAB™ . The magnitude response plot of the various filters used in this block diagram are studied on MATLAB™ and depending upon their performance under various sinusoidal and non-sinusoidal conditions various trail and errors were performed to finalize the order and type of filters.

The input signal is sampled by the ADC block, ADC block converts the analog voltage signal into digital samples values, which are further filtered by band pass filter as shown in the Fig.2.4-1.

The Band pass filter used is a 40 order FIR (Finite Impulse Response) filter with a pass band frequency range from 30 to100Hz. The time required to reach steady state is 2 cycles due to 40 order filter increasing the order will increase the time to reach steady state. The design details of the filter are given in Table 2.4-1.

Sr.No	Design Parameter	Design Method
1.	Structure	Direct-Form FIR
2.	Order	40
3.	Type	Band pass
4.	Design Method	FIR-Window
5.	Window	Kaiser
6.	Beta	0
7.	Sampling Frequency	1000
8.	Band Pass Band	30-100 Hz

Table 2.4-1 Design details for the Band Pass filter

As shown in the Fig. 2.4-2, Fig. 2.4-3 and Fig. 2.4-4 the magnitude, phase and impulse response of the band pass filter

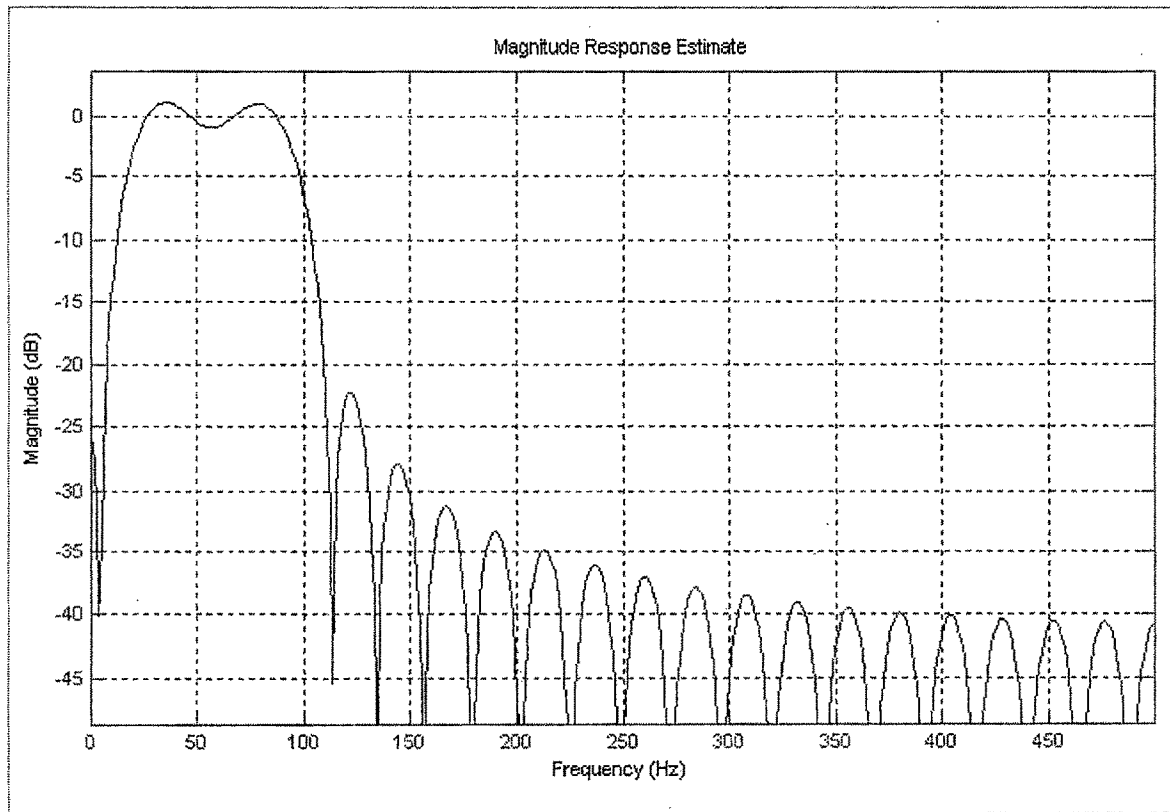


Fig. 2.4-2 Magnitude response of band pass filter

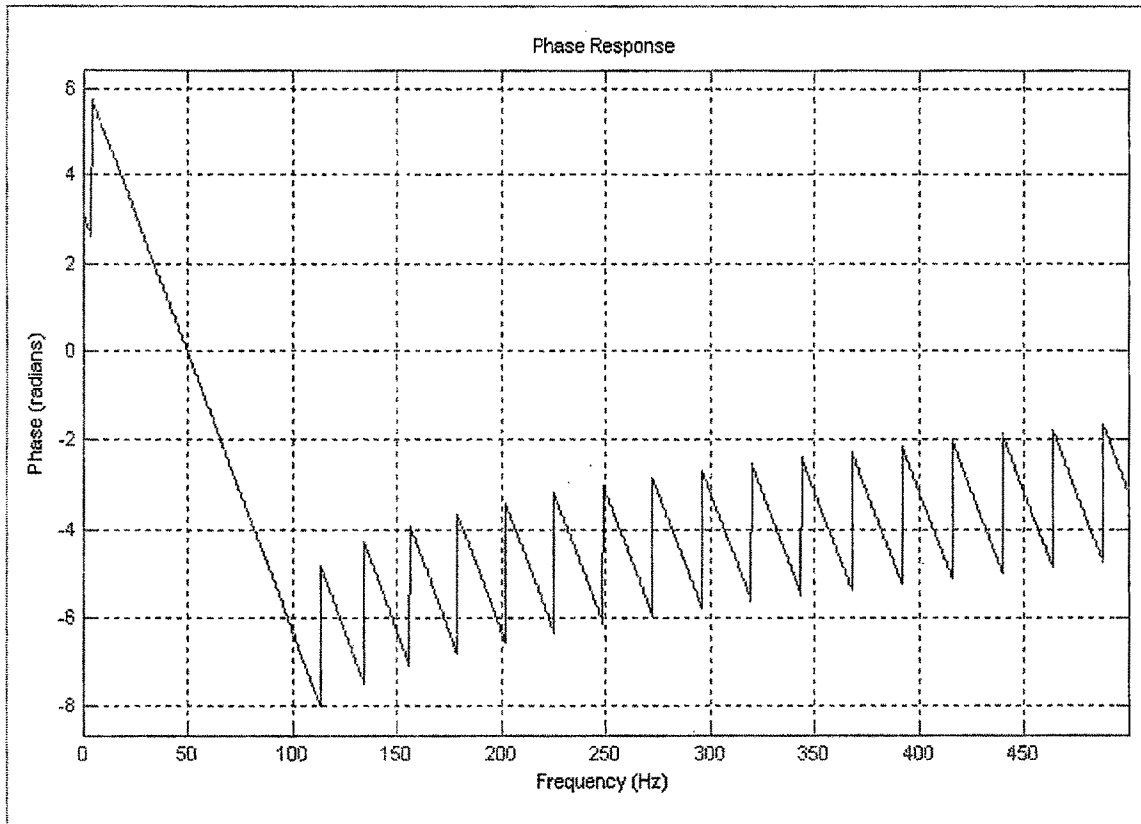


Fig. 2.4-3 Phase response of band pass filter

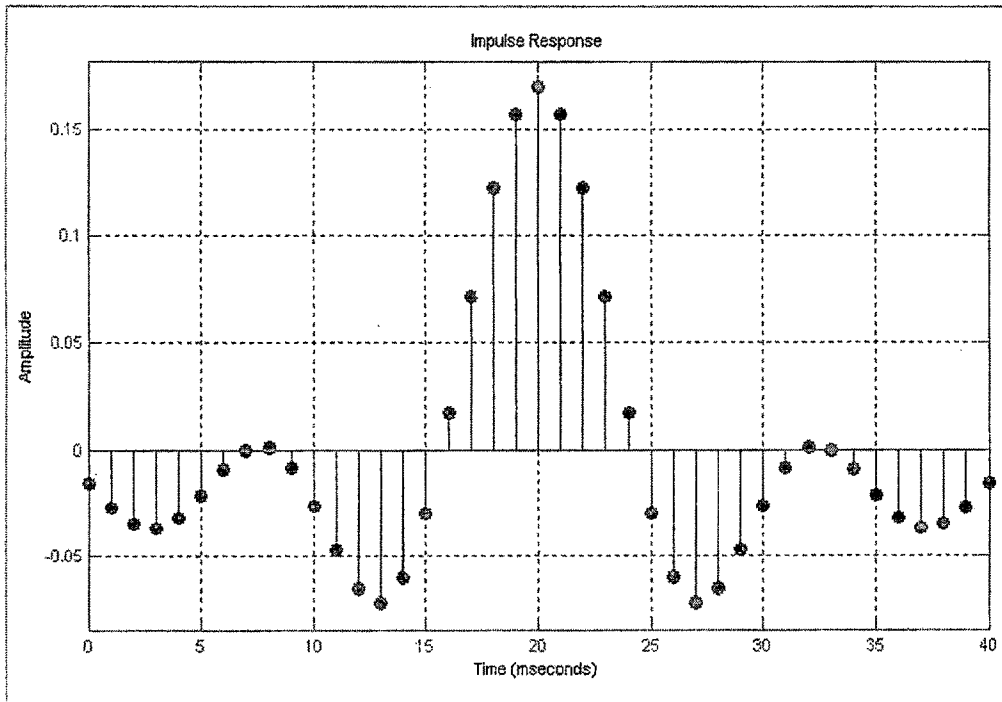


Fig. 2.4-4 Impulse Response of filter

Discrete-Time FIR Filter (real)	0.01748
	0.07131
% Filter Structure : Direct-Form FIR	0.12154
	0.15714
% Filter Length : 41	0.17
% Stable : Yes	0.15714
% Linear Phase : Yes (Type 1)	0.12154
	0.07131
Numerator:	0.01748
-0.0151	-0.0289
-0.0262	-0.0596
-0.0344	-0.0711
-0.0365	-0.0651
-0.0315	-0.0473
-0.021	-0.0258
-0.0087	-0.0079
0.00025	0.00123
0.00123	0.00025
-0.0079	-0.0087
-0.0258	-0.021
-0.0473	-0.0315
-0.0651	-0.0365
-0.0711	-0.0344
-0.0596	-0.0262
-0.0289	-0.0151

Tab.2.4-2 Co-efficient of the Band Pass filters

The other two filters used in blocks are FIR filters, they are mainly low pass and all-pass filters. Both the filters are digitally designed in such a way that the phase angle change to the input signal is same for both the cases. The design details of both the filters are given in Table 2.4-3. The amplitude and phase response of the low pass FIR filter is given in Fig. 2.4-5 and Fig. 2.4-6. The coefficients of the LPF and FIR filter are given in Table 2.4-4 and Table 2.4-5. Similarly the amplitude and phase response of the all pass FIR filter is given in Fig. 2.4-8 and Fig. 2.4-9. The impulse response of the filters are given in Fig. 2.4-7 and Fig. 2.4-10.

Design details of the FIR low pass and all pass filter

Sr.No	Parameter	Design	Low Pass	High Pass
1	Structure	Direct Form FIR		
2	Order	NA	10	10

Table 2.4-3

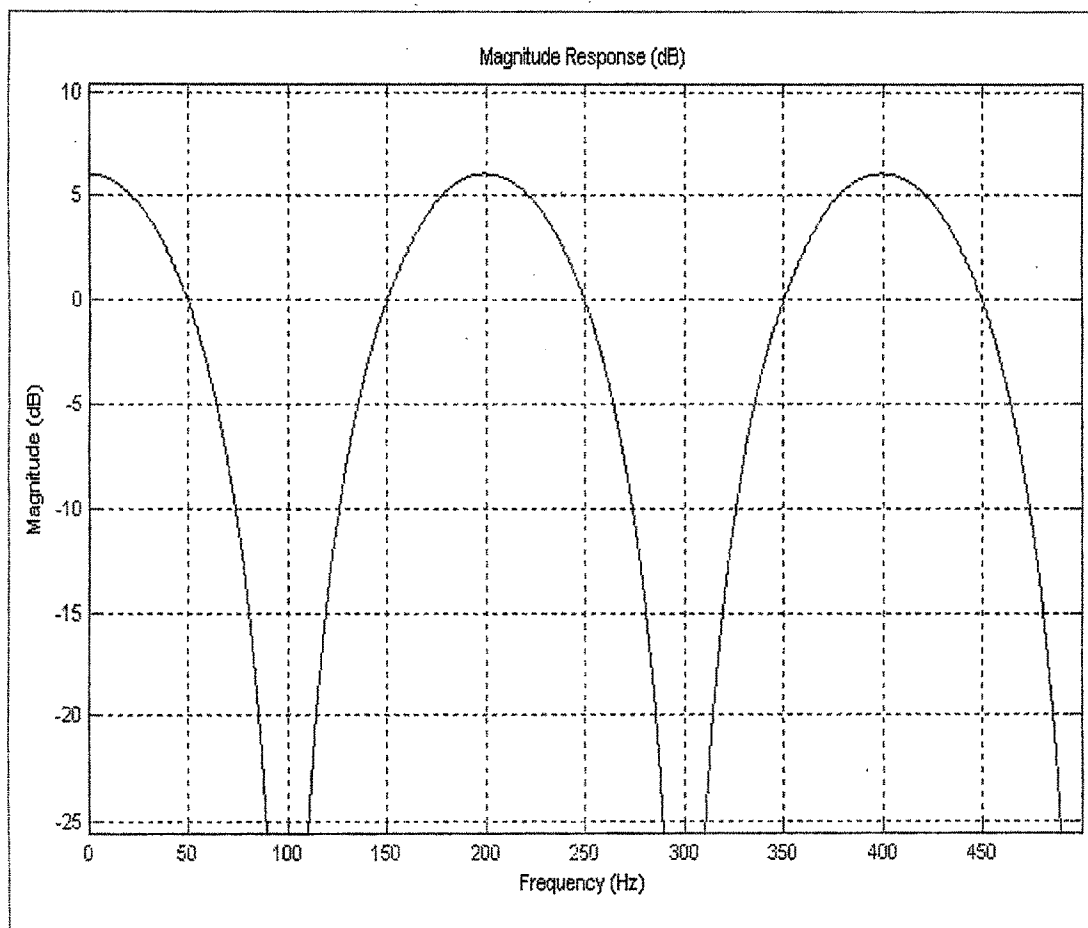


Fig. 2.4-5 Amplitude response of the Low Pass Filter

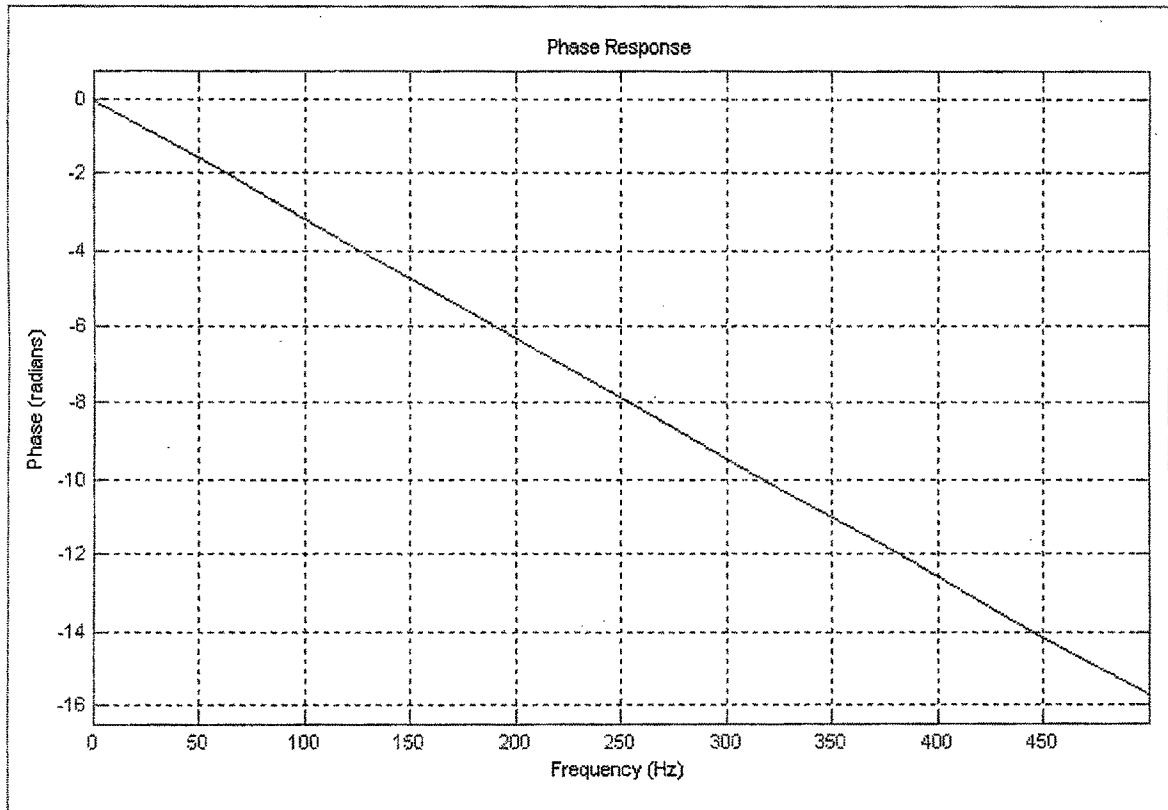


Fig. 2.4-6 Phase response of the Low Pass Filter

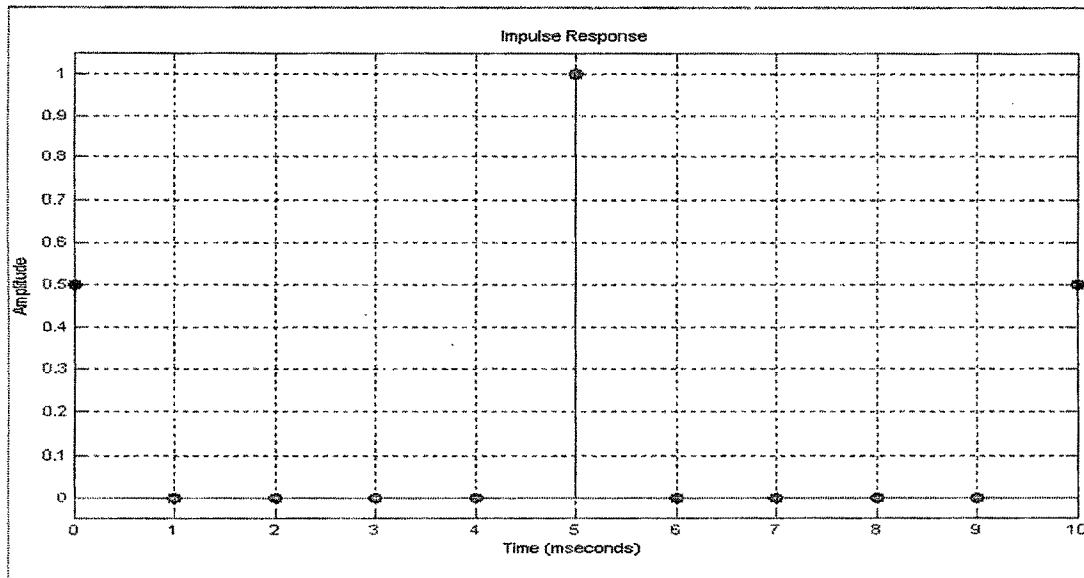


Fig. 2.4-7 Impulse Response of the Low Pass Filter

% Coefficient Format: Decimal
% Discrete-Time FIR Filter (real)
% Filter Structure : Direct-Form FIR
% Filter Length : 11
% Stable : Yes
% Linear Phase : Yes (Type 1)
Numerator:
0.5
0
0
0
0
1
0
0
0
0
0
0.5

Table 2.4-4 Coefficients of Low Pass filters

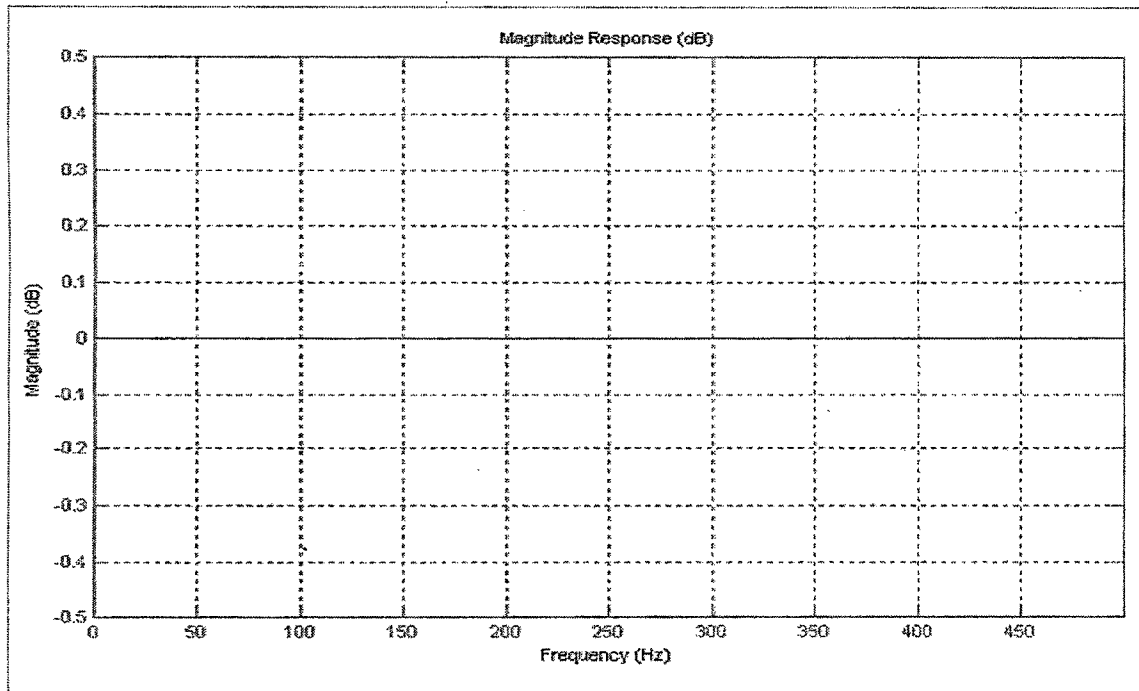


Fig. 2.4-8 Amplitude response of the All Pass Filter

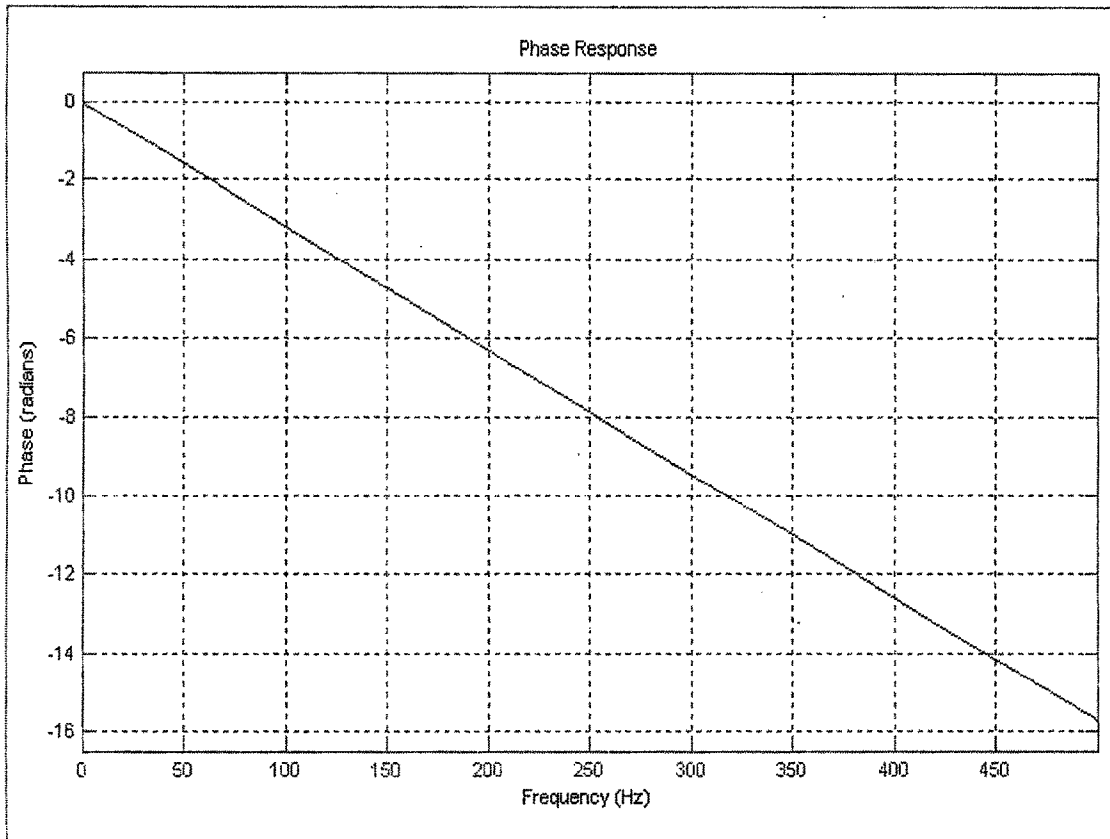


Fig. 2.4-9 Phase response of the All Pass Filter

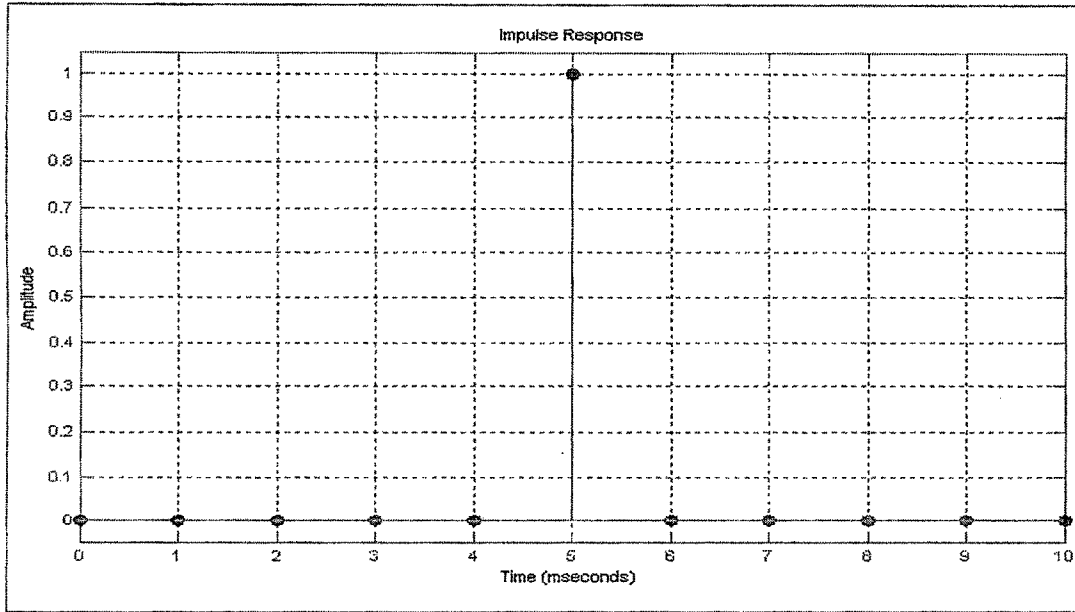


Fig. 2.4-10 Impulse Response of the Low Pass Filter

% Coefficient Format: Decimal	
% Discrete-Time FIR Filter (real)	
% Filter Structure : Direct-Form FIR	
% Filter Length : 11	
% Stable : Yes	
% Linear Phase : Yes (Type 1)	
Numerator:	
	0
	0
	0
	0
	0
	1
	0
	0
	0
	0
	0

Table 2.4-5 Coefficients of the All Pass Filter

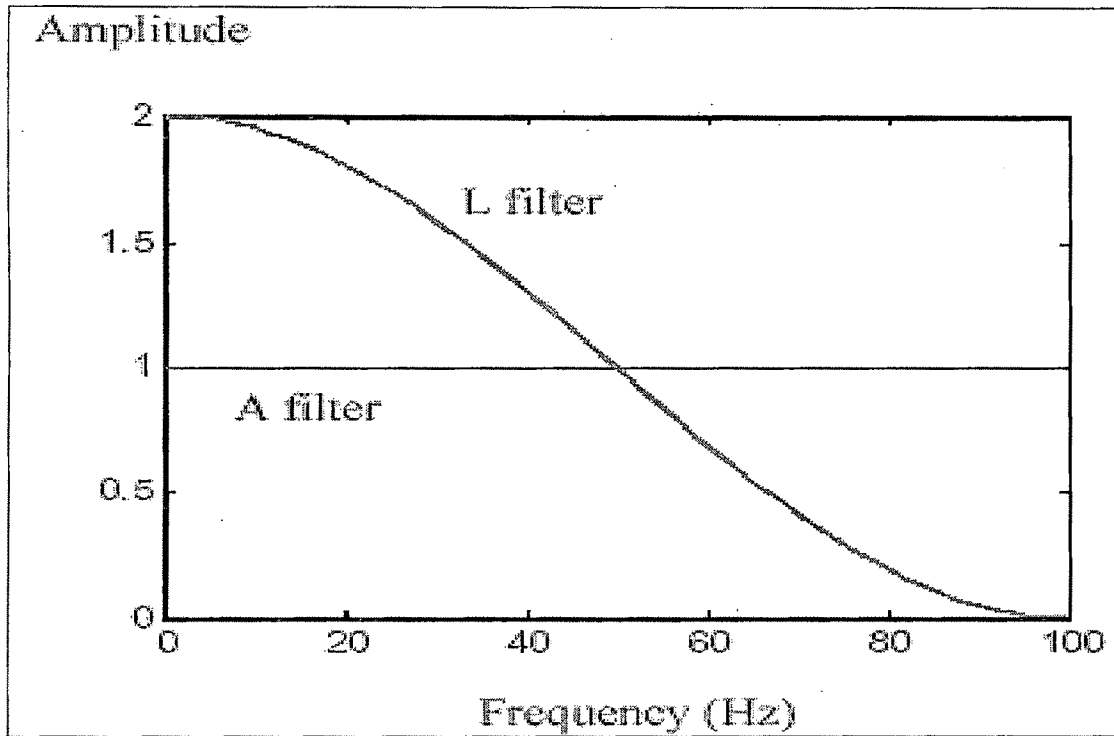


Fig. 2.4-11 Amplitude and Frequency response of the LPF and APF

The digital instantaneous values of the voltage signal are processed through band-pass and then through all-pass and low pass filters whose design and the response of the filters were explained in the previous section.

After passing the instantaneous values through the low pass and all pass filter the instantaneous values are then processed through an IIR filter. The IIR filter is designed using the Eq. 2.11. The design of IIR filter is not covered in Sezi Model [12]. The IIR filter is required to obtained a value proportional to signal amplitude.

$$y_c [n] = y_c [n - 1] + 0.1(x_c^2[n] - x_c^2[n - 10]) \quad (2.11)$$

Where

y_c Is IIR filter output

x_c Is input filter data values

2.5 Mathematical Analysis

The sample data $x[n]$ is first filtered by a band pass FIR filter with the pass band frequency range from 30 to 100 Hz. The filter suppress sub harmonic and high frequency signal to about 25dB with respect to the input signal being present. The band pass filter is a two-cycle FIR Fourier filter with rectangular window. The output of the band pass-filter is connected to two other filters. One of them is an all pass-filter (A-filter), which changes the phase angle, but not the amplitude, of the signal. The other filter is a low-pass filter (L-filter) that changes amplitude of the signal, while changing phase angle of the signal in exactly same way as the A-filter. Both low pass and all pass are FIR filters and are designed with the Eq. 2.12.

$$y(k) = a_0x(k) + a_1x(k - 1) + \dots + a_Mx(k - M) \quad (2.12)$$

Where $y(k)$ is the output of the filter, $x(k)$ is the latest data sample value, $x(k - 1)$ is the previous data sample value, up to the M^{th} previous data sample, $x(k - M)$ and a_0 to a_M are the bandpass filter co-efficients . The time interval between the samples is determined by the sampling frequency f_s . The value of M is the order of filter. The influence of each data samples value on the output of the filter is determined by the filter's coefficients a_0, a_1, \dots, a_M . Both the low pass and high pass filters have end-to end symmetrical pattern. The first and last

coefficients are equal; second and next-to-last coefficients are equal and so on: $a_0 = a_M, a_1 = a_{M-1}, a_2 = a_{M-2}$ etc. Both filters described in the paper have (M+1) number of coefficients, where M is the order of filter. Since the filter order is 10, these filters have 11 numbers of coefficients. All the coefficients of the A-filter are zero except $a_{M/2} = 1$. Whereas in case of L-filter the coefficients are $a_0 = 0.5$ and $a_M = 0.5$ with other coefficients=0.

For sinusoidal signals, the filters performance defined by the Eq. 2:13

$$Y(j\Omega) = H(j\Omega)X(j\Omega)$$

Where $H(j\Omega)$ are the filter coefficients and $X(j\Omega)$ are the samples of the input signal to the filter

$$H(j\Omega) = \left[a_{M/2} + 2 \sum_{k=0}^{\frac{M}{2}-1} a_k \cos \left[\left(\frac{M}{2} - k \right) \Omega \right] \right] e^{-j\Omega(M/2)} \quad (2.13)$$

Where Ω is the normalized frequency.

The A-filter is an all-pass filter with phase and amplitude response given by Eq. 2.14

$$A(j\Omega) = A(\Omega)e^{-j5\Omega} \quad A(\Omega) = 1 \quad (2.14)$$

The L-filter is a low-pass filter with phase and amplitude response given by Eq. 2.15.

$$L(j\Omega) = (1 + \cos(5\Omega))e^{-j5\Omega} \quad L(\Omega) = (1 + \cos(5\Omega)) \quad (2.15)$$

As shown in Fig. 2.4-11 the amplification factor of the L-filter and A-filter are equal at nominal line frequency. In general the frequency functions of both filters are given by Eq. 2.16 and 2.17.

Low pass filter

$$L(f) = 1 + \cos(5\Omega) \quad (2.16)$$

All pass filter:

$$A(f) = 1 \quad (2.17)$$

Where

$$\Omega = 2\pi \left(\frac{f}{f_s} \right) \quad (2.18)$$

Ω is the normalized frequency.

f Is the actual frequency.

f_s Sampling frequency.

The outputs of the filter A and L pass through an IIR (Infinite Impulse Response) filter. The IIR filter provide X_L and X_A as the signal amplitude corresponding to the input from L-filter and A-filter.

The divide block computes the quotient of the signals X_L and X_A . This ratio corresponds to the known ratio of the frequency dependent amplification factors of the filters $L(\Omega)$ and $A(\Omega)$.

$$\frac{X_L}{X_A} = [1 + \cos(5\Omega)] \quad (2.19)$$

The frequency calculation block performs a root squared of divider output and then perform the inverse of the cosine function to calculate the value of Ω .

$$\Omega = \frac{1}{5} \arccos \left[\left(\frac{x_L}{x_C} \right) - 1 \right] \quad (2.20)$$

The output of the frequency calculation block is the actual line frequency given by Eq. 2.21

$$f = \frac{f_s \Omega}{2\pi} \quad (2.21)$$

If actual frequency is nominal frequency, the amplitudes of the signals output by filters A and L will be equal. If actual frequency is lower than nominal frequency, signal output of filter L will have higher amplitude than signal output of filter A. If actual frequency is higher, output of filter L will be lower than the value of filter A.

Because the same numerical process is used to calculate the signal amplitude and quotient of amplitudes, all frequency dependent errors are eliminated. The algorithm is only sensitive to numerical accuracy of processor. Now a day's 32-bit floating-point processor are easily available with internal analog to digital converter. So a single controller can accurately compute the line frequency

2.6 Extension to Three-Phase System

Since, frequency measurement is one of the critical parameter in single phase and three phase system. The proposed model for single phase is also extended for three phase system. In case of three phase system, proposed method can be

implemented on any one phase. But due to non-availability of voltage on that phase due to disturbance (blown fuse), frequency cannot be determined. Thus in case of three phase voltage, frequency measurement is based on determining reference voltage phasor using the instantaneous α - β theory[30] as described in Eq. 2.22 and Eq. 2.23 . The block diagram of frequency measurement for three phase system is given in Fig. 2.6-1.

$$V_{\alpha} = 0.816 * V_a - 0.41 * V_b - 0.41 * V_c \quad (2.22)$$

$$V_{\beta} = 0.707 * V_b - 0.707 * V_c \quad (2.23)$$

The Reference voltage phasor magnitude and angle is given b y Eq. 2.24

$$V = \sqrt{(V_{\alpha}^2 + V_{\beta}^2)} \quad \phi = \tan^{-1}\left(\frac{V_{\beta}}{V_{\alpha}}\right) \quad (2.24)$$

Where V_a, V_b and V_c are three phase voltages.

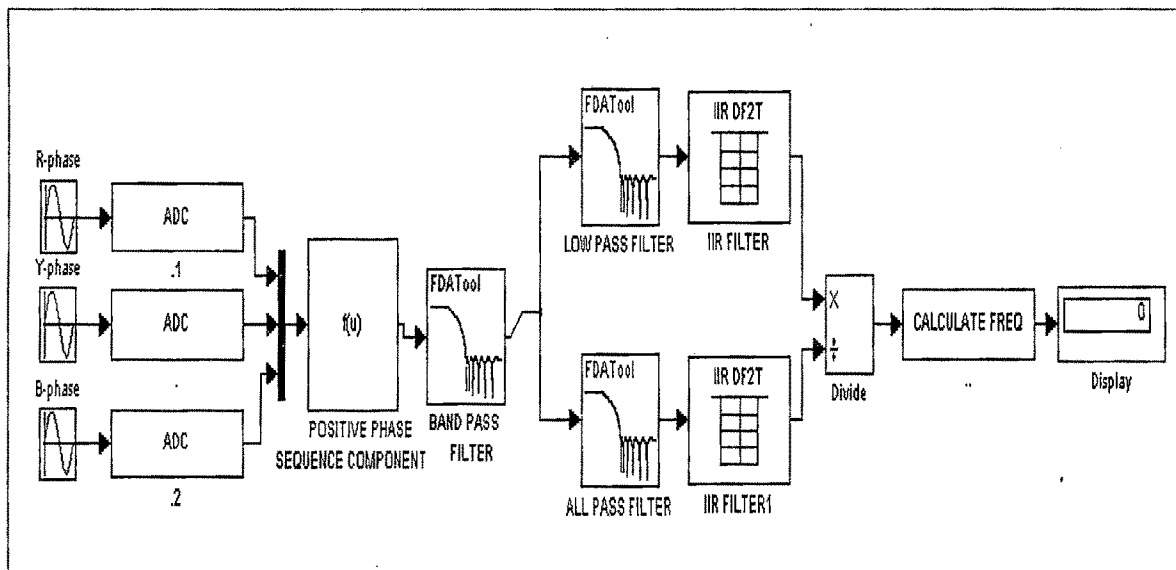


Fig. 2.6-1 Block diagram of frequency measurement for three phase

As shown in the block diagram the three phase input signals are sampled by the ADC channels and from the sampled values the positive sequence signal is computed, the computed signal is then processed to the band-pass filter, the output of the bandpass filter is then processed to the low pass and all pass filter. The remaining processing is just similar to the single phase component.

2.7 Simulation Results

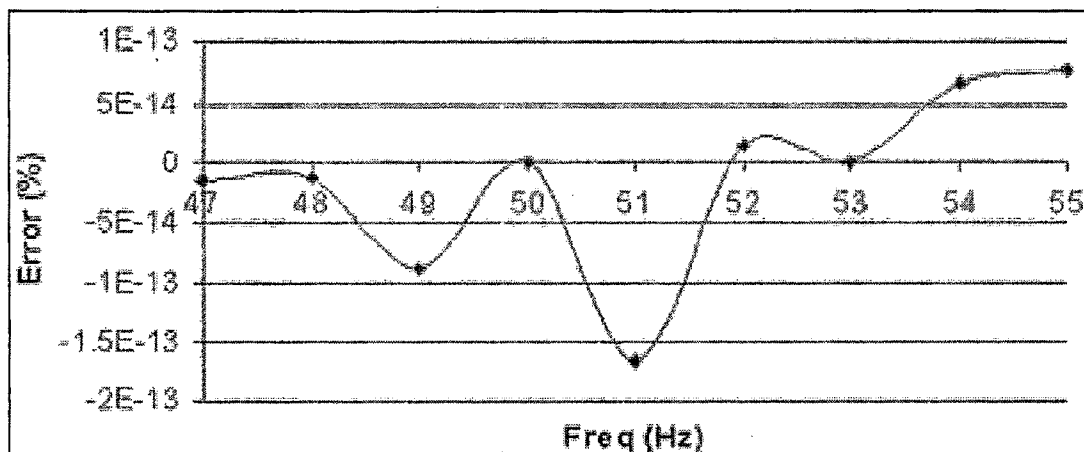
The method was also tested under sinusoidal and non-sinusoidal conditions. It shows excellent accuracy under both conditions.

2.7.1.1 Simulation On Excel

❖ Case -1

In sinusoidal condition, voltage signals were given to the proposed method. The errors achieved at various frequencies are plotted under sinusoidal conditions. Fig. 2.7-1 shows the error under sinusoidal conditions. From the result it is shown that the maximum error under sinusoidal conditions is 5×10^{-15} . Thus shows the excellent response under sinusoidal conditions.

Fig. 2.7-1 Error under sinusoidal conditions



❖ **Case -2**

Methodology Tested under various harmonic conditions. The third, fifth and seventh harmonic signal is added in phase with fundamental signal. The combined signal is sampled and applied through proposed method. The error of frequency from 47Hz to 55Hz at 30% of third harmonic, 20% of fifth harmonic and 20% of seventh harmonic are plotted as shown in Fig. 2.7-2. The results shows that the maximum error achieved under these conditions are 0.02%.

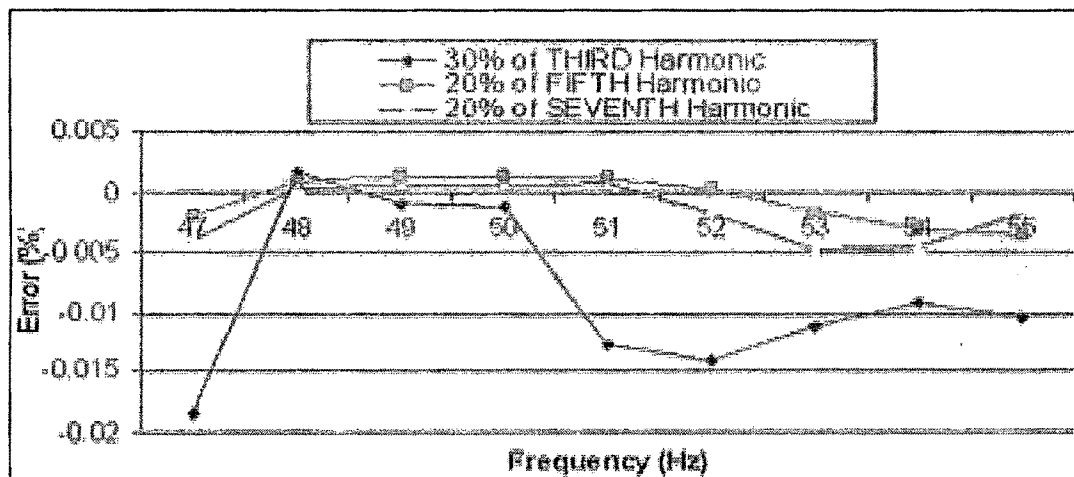


Fig. 2.7-2 Error under harmonic conditions

❖ **Case -3**

Methodology was tested for signals with multiple zero crossing frequency. The test signal was as shown in Fig. 2.7-3. The method shows no abnormalities under multiple zero crossing conditions.

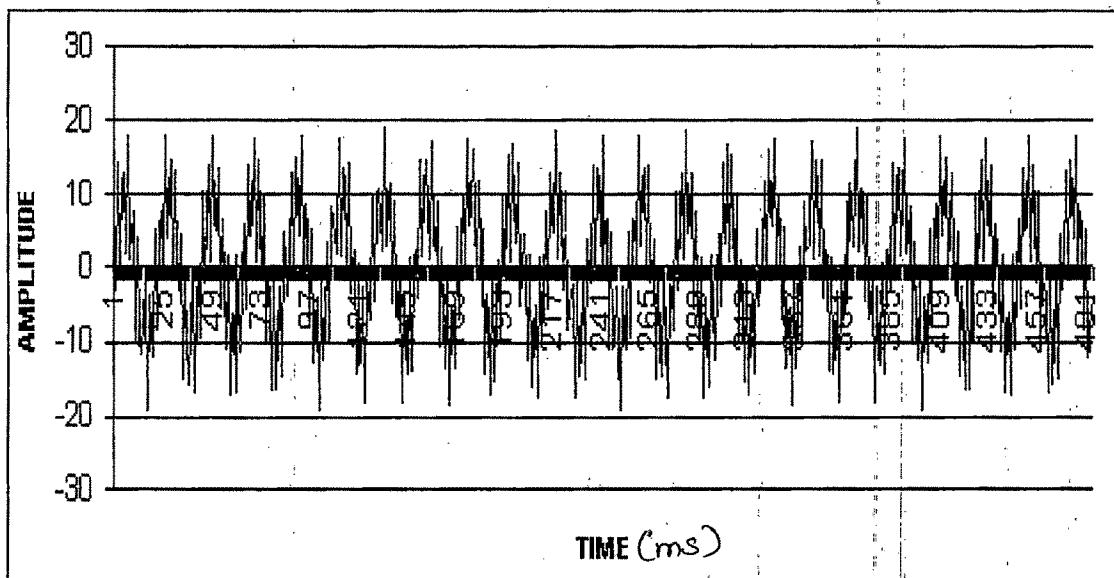


Fig. 2.7-3 Signal with multiple zero crossing.

This proves that proposed method is independent of zero crossing of input signal. Input signal with various frequencies and multiple zero crossing were tested with proposed method. The maximum error achieved is -0.005% at 53Hz frequency as shown in Fig. 2.7-4.

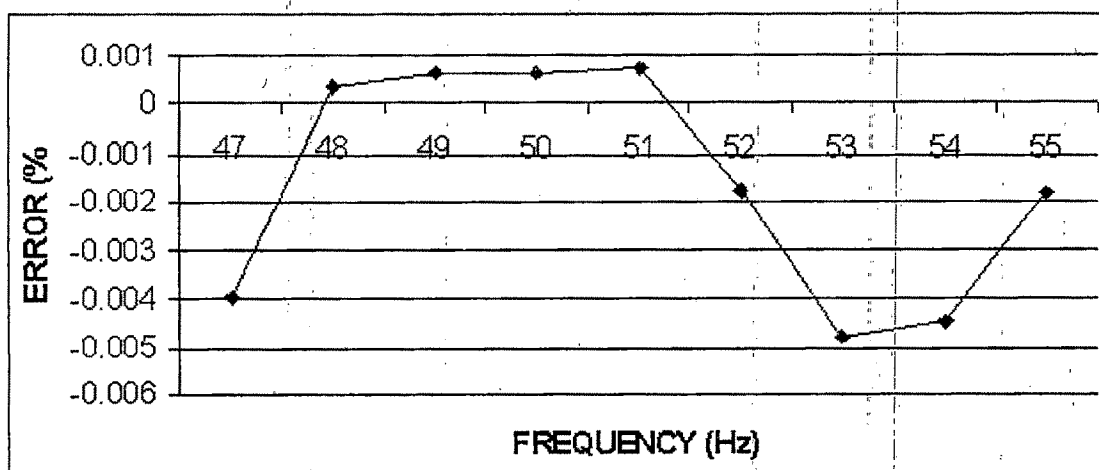


Fig. 2.7-4 Error with multiple zero crossing.

❖ Case -4

The proposed method is tested under various harmonic conditions. The harmonic content in fundamental voltage is varied from 1% to 50% of the fundamental voltage. Fig. 2.7-5 shows the plot for error v/s harmonic content added to fundamental.

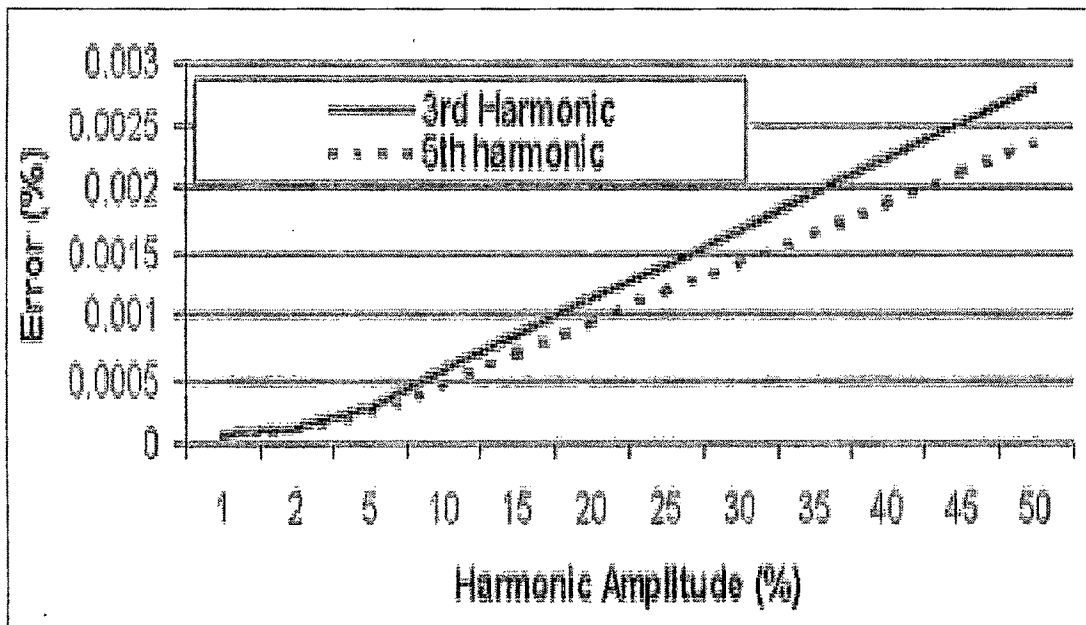


Fig. 2.7-5 Error with various harmonic content.

❖ Case -5

There is a possibility of sub harmonic signal being present in the fundamental signal. In such case the proposed method is tested when sub harmonic signal (i.e. 1/3 of the fundamental frequency) is present in fundamental signal. The maximum error obtained in this case is 0.8%. Fig. 2.7-6 shows the plot at various frequencies along with 1/3rd of the fundamental frequency component signal presence.

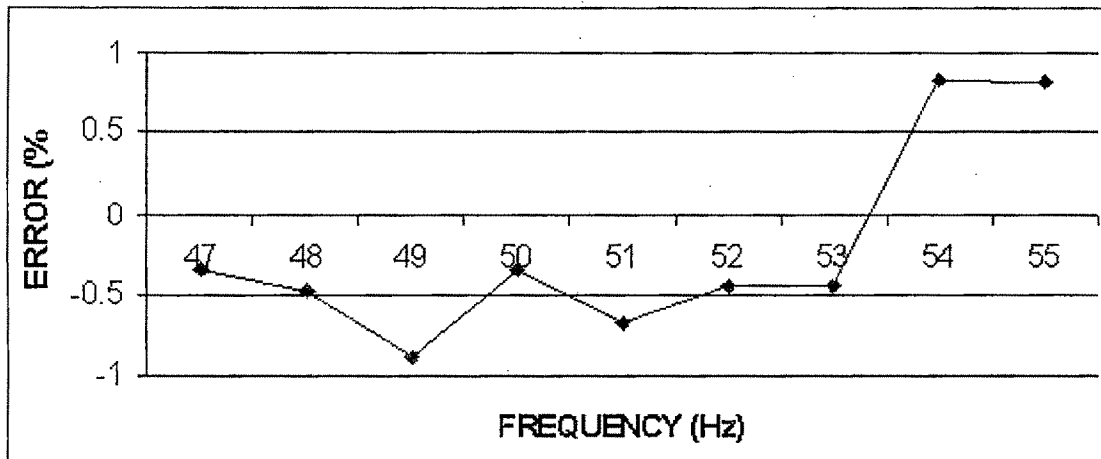


Fig. 2.7-6 Error in case of sub harmonic condition.

2.7.2 Simulation On Matlab™

In order to test the suitability of system, proposed method is also simulated on MATLAB™ software. In this case, GUI (Graphic user interface) model of MATLAB™ is developed so that the system could be tested for various cases and under sinusoidal and non-sinusoidal conditions. All the filter equations are modeled in the M-file and the complete model is converted into the source code as shown in Fig. 2.7-7. The various input parameters to run the model are given through GUI window, such as input voltage, frequency, and harmonics. The models display the calculated frequency on the screen after computation. In order to reduce the complexity and poor visibility only one phase voltage signal is displayed on the screen. As described earlier the time required by the system to reach the steady state is 3 cycles.

❖ **Case -1-Freq Measurement Under Sinusoidal Condition**

As described in the previous excel simulation the model is initially tested under sinusoidal conditions at various frequencies. The screen shots are shown in Fig. 2.7-7. Table 2.7.1 shows simulation results under sinusoidal conditions. The plot of the error obtained at various frequencies is given in Fig. 2.7-8.

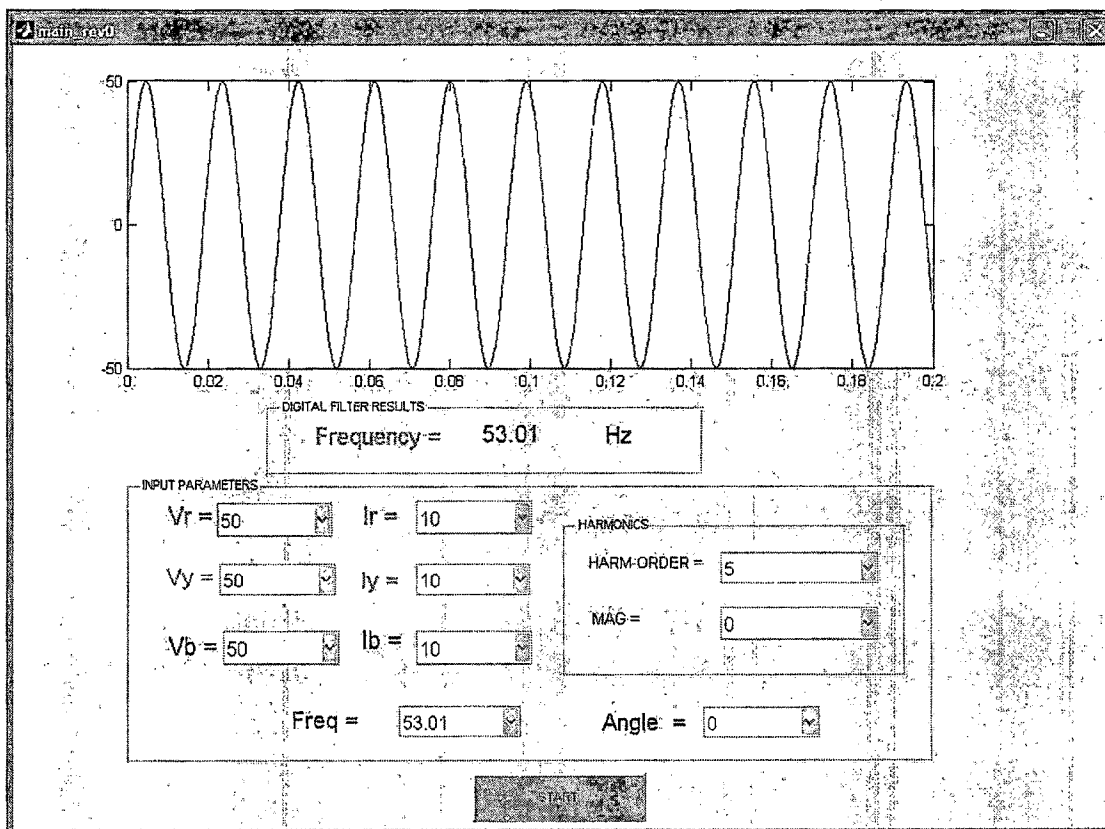


Fig. 2.7-7 Simulation results for case 1

Condition: Sinusoidal Conditions			
Sr.No	Actual Frequency (Hz)	Measured Frequency (Hz)	Error (%)
1	46.12	46.1209	-0.00195
2	46.54	46.5401	-0.00021
3	47.08	47.0802	-0.00042
4	48.97	48.9703	-0.00061
5	49.99	49.9901	-0.0002
6	50	50.0001	-0.0002
7	51.1	51.1001	-0.0002
8	52.29	52.2901	-0.00019
9	53.01	53.0103	-0.00057
10	54.95	54.9501	-0.00018

Table 2.7-1 Comparison under sinusoidal conditions

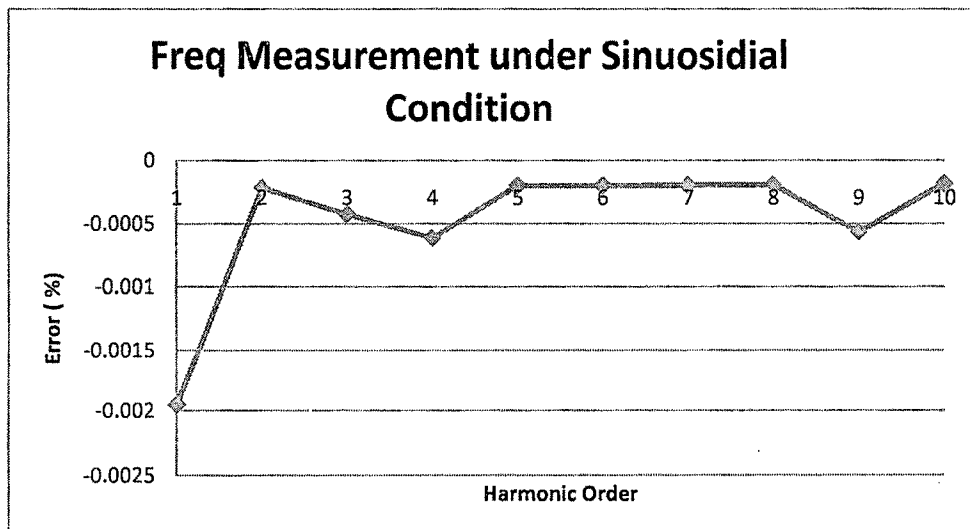


Fig. 2.7-8 Comparison results for frequency measured under sinusoidal conditions

❖ **Case -2 Freq Measurement Under Harmonic Condition**

In this case the proposed model is tested by inserting harmonics of various orders. The system is tested by keeping input frequency constant and increasing the magnitude of harmonics from 5% to 50% of voltage signal for various order such as third, fifth up to twenty fifth order of harmonic.. The screen shots are shown in Fig. 2.7-9. Table 2.7.2 shows various simulation results under harmonic conditions. The plot of error obtained at various frequencies is given in Fig. 2.7-10.

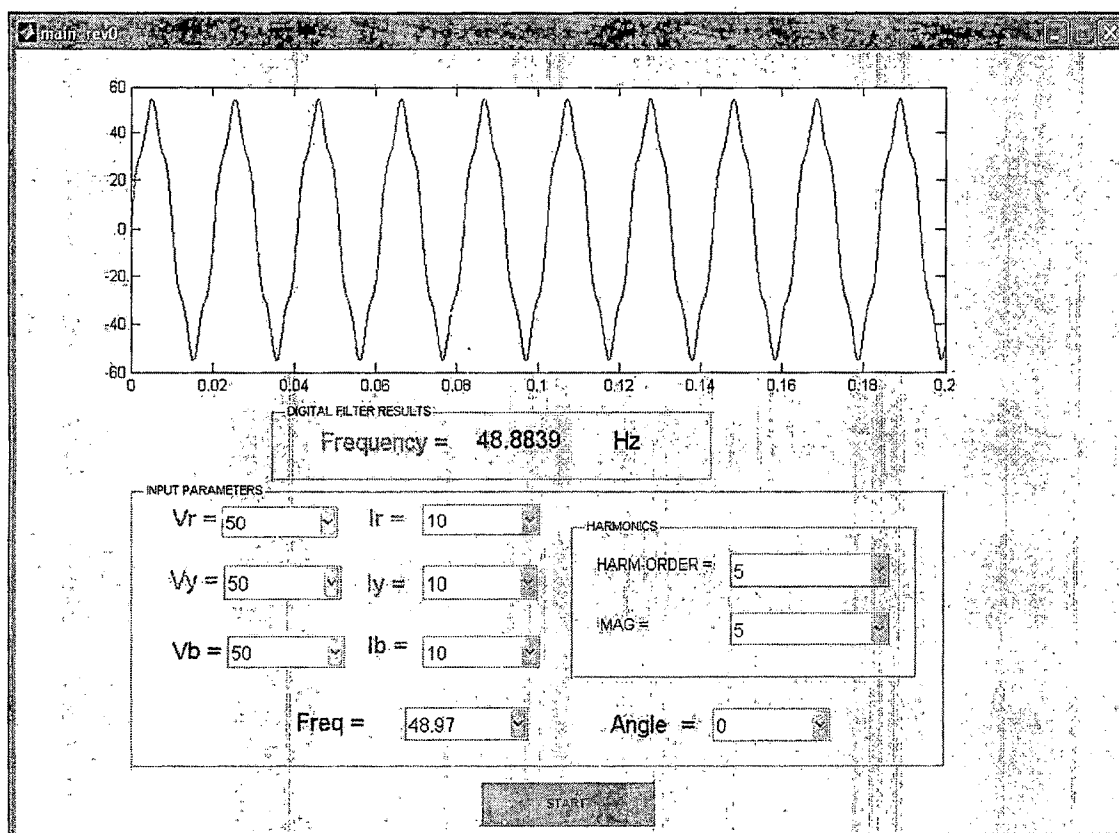


Fig. 2.7-9

Results of the freq measurement for 5th harmonic for 5% of the fundamental value

Condition: Harmonic Conditions at 5% of the Input voltage				
Sr.No	Actual Frequency (Hz)	Measured Frequency (Hz)	Harmonic Order	Error (%)
1	49.99	49.9915	3	-0.003
2	49.99	49.9894	5	0.0012
3	49.99	49.9889	7	0.0022
4	49.99	49.9891	9	0.0018
5	49.99	49.9881	11	0.003801
6	49.99	49.9878	13	0.004401
7	49.99	49.9884	15	0.003201
8	49.99	49.9863	17	0.007401
9	49.99	49.982	19	0.016003
10	49.99	49.9814	21	0.017203
11	49.99	50.0079	23	-0.03581
12	49.99	49.9802	25	0.019604

Table 2.7-2 Table Results of Frequency Measured under 5% of Harmonic in voltage Signal

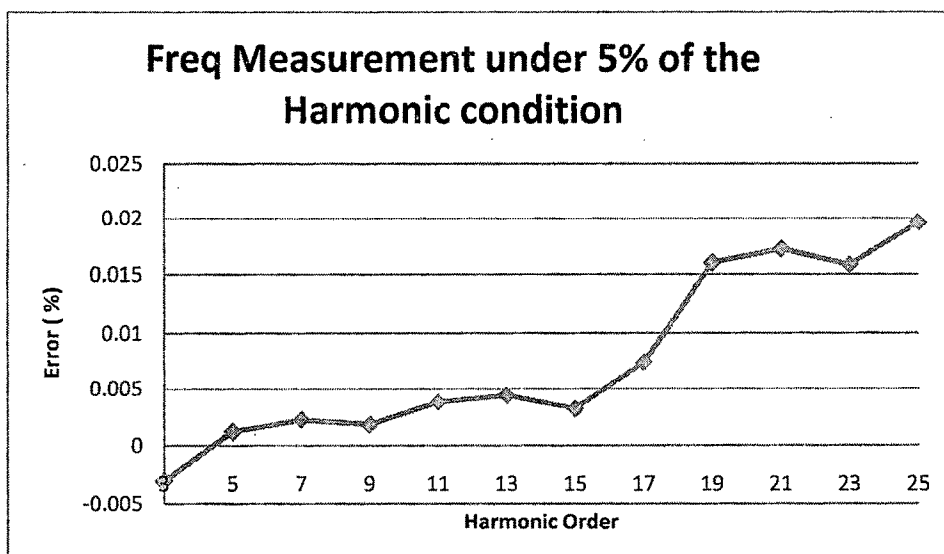


Fig. 2.7-10 Comparison results for frequency measured by inserting 5% of Harmonic in fundamental signal

The screen shots of 25% of harmonic in fundamental signal are shown in Fig. 2.7-11. A table of the various simulation results under harmonic conditions is given in Table 2.7-3. The plot of the error obtained at various frequencies is given in Fig. 2.7-12.

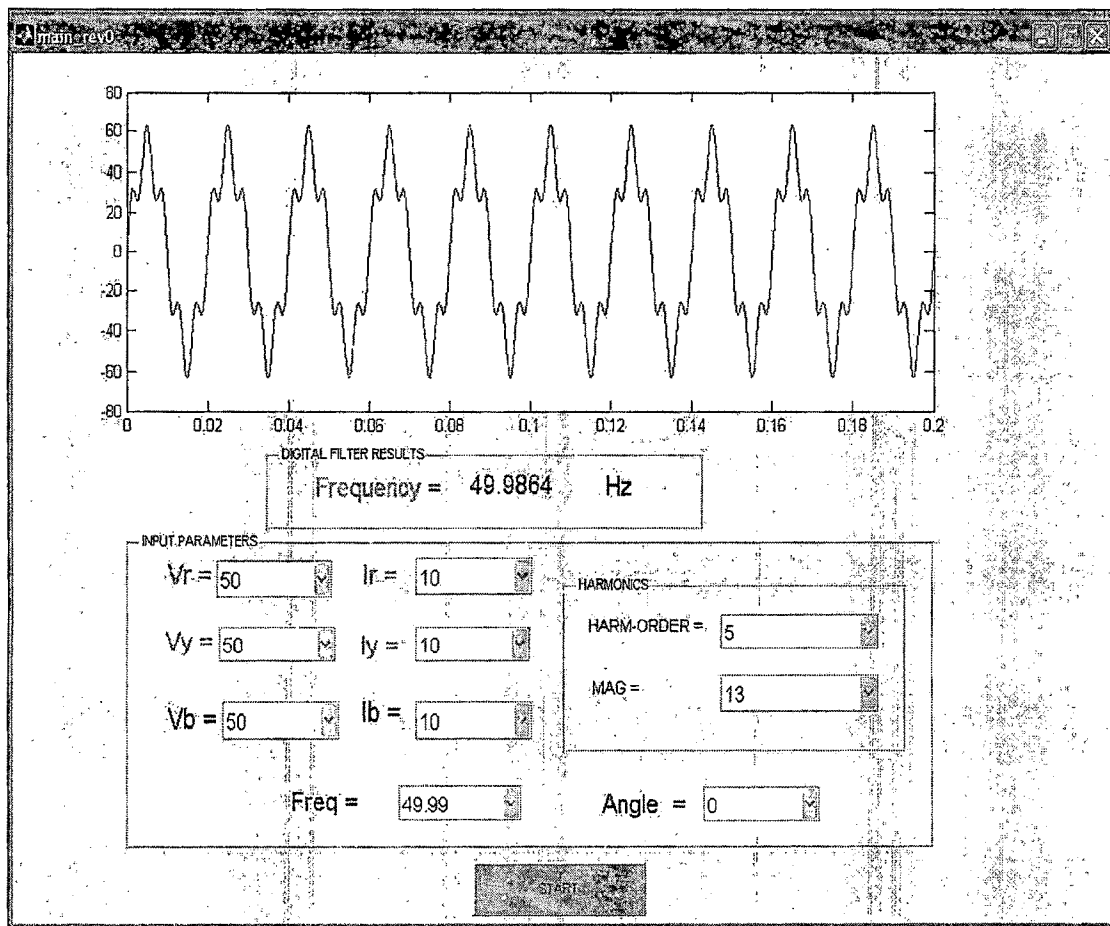
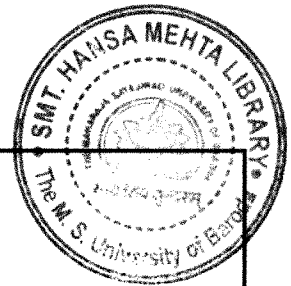


Fig. 2.7-11 Results of the freq measurement for 5th harmonic for 25% of the fundamental value



Condition: Harmonic Conditions at 25% of the Input voltage				
Sr.No	Actual Frequency (Hz)	Measured Frequency (Hz)	Harmonic Order	Error (%)
1	49.99	49.9936	3	-0.0072
2	49.99	49.9886	5	0.002801
3	49.99	49.987	7	0.006001
4	49.99	49.9879	9	0.004201
5	49.99	49.9879	11	0.004201
6	49.99	49.9852	13	0.009602
7	49.99	50.0045	15	-0.02901
8	49.99	49.9863	17	0.007401
9	49.99	50.2143	19	-0.44869
10	49.99	49.8066	21	0.366873
11	49.99	50.0193	23	-0.05861
12	49.99	49.9743	25	0.031406

Table 2.7-3

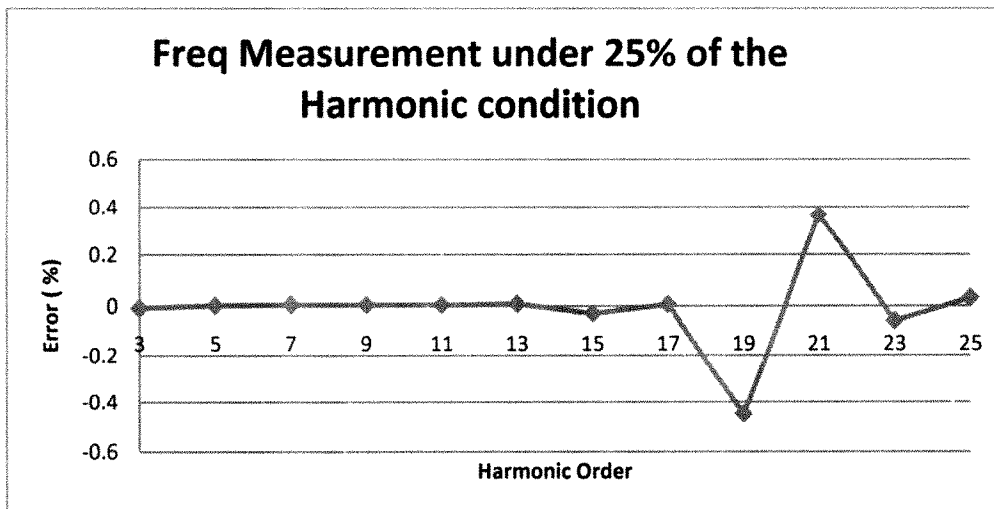


Fig. 2.7-12

Comparison results for frequency measured by inserting 25% of Harmonic in fundamental signal

The screen shots of 50% harmonic in fundamental signal are shown from Fig. 2.7-13. A table of the various simulation results under harmonic conditions is given in Table 2.7-4. The plot of error obtained at various frequencies is given in Fig. 2.7-14.

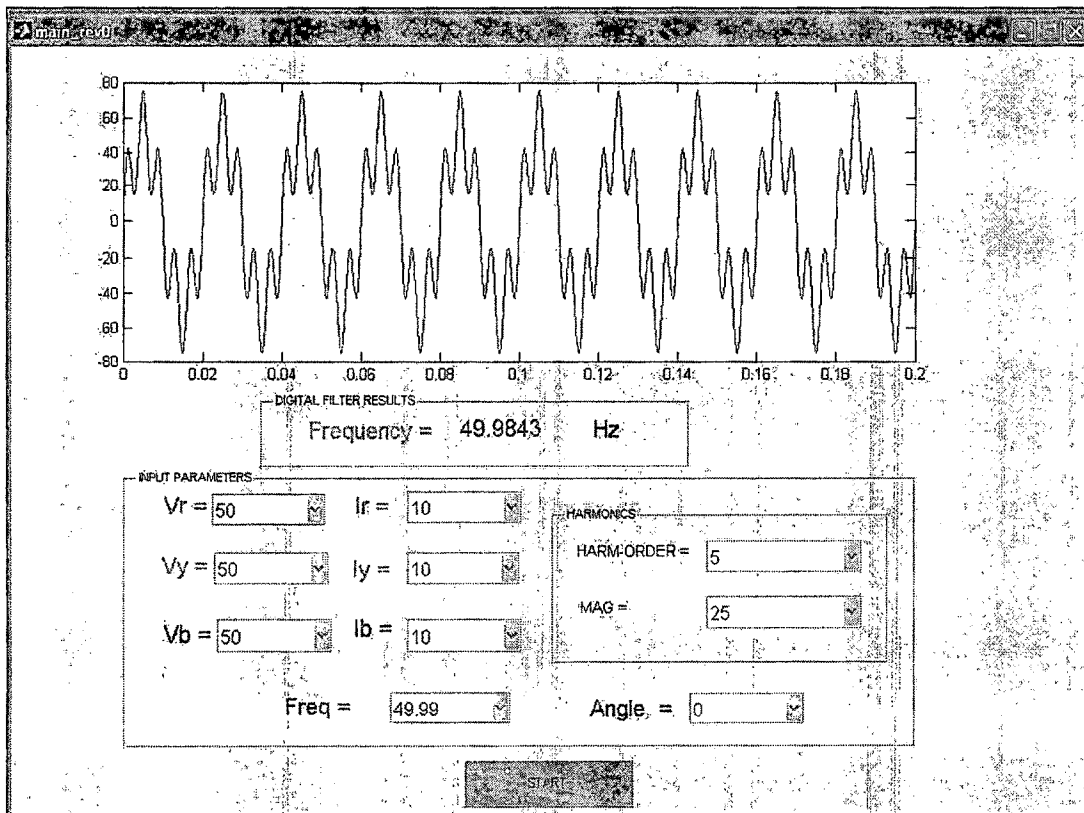


Fig. 2.7-13

Results of the freq measurement for 5th harmonic for 50% of the fundamental value

Condition: Harmonic Conditions at 50% of the Input voltage				
Sr.No	Actual Frequency (Hz)	Measured Frequency (Hz)	Harmonic Order	Error (%)
1	49.99	49.996	3	-0.012
2	49.99	49.9876	5	0.004801
3	49.99	49.983	7	0.014003
4	49.99	49.9864	9	0.007201
5	49.99	49.9685	11	0.043009
6	49.99	49.9824	13	0.015203
7	49.99	49.9895	15	0.001
8	49.99	50.0392	17	-0.09842
9	49.99	50.2009	19	-0.42188
10	49.99	49.7992	21	0.381676
11	49.99	50.032	23	-0.08402
12	49.99	49.9685	25	0.043009

Table 2.7-4

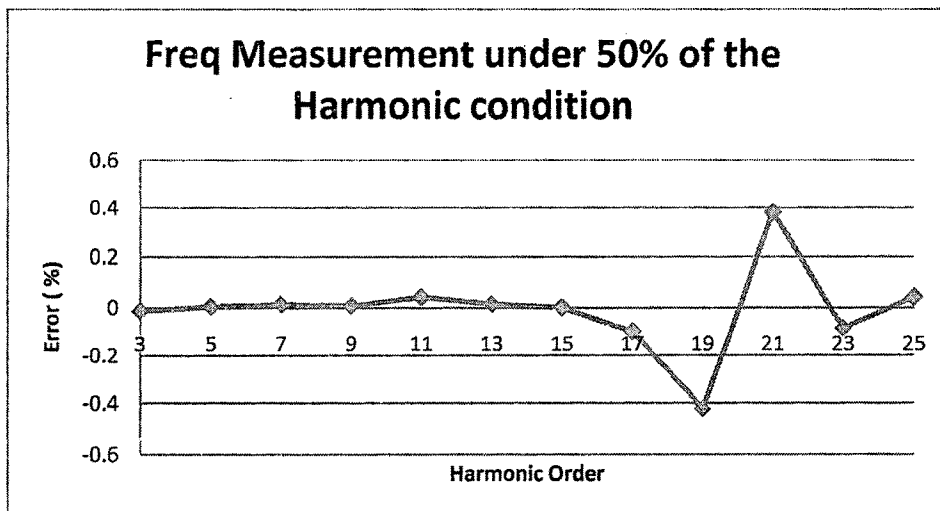


Fig. 2.7-14
Error Obtained at 50% of the harmonic

❖ **Case -3 Freq Measurement Under Multiple Zero Crossing Condition**

As shown in Fig. 2.7-15 the system is able to measure frequency in case of the multiple zero crossing and noisy conditions. This indicates that suitability of system for noisy and harmonic conditions.

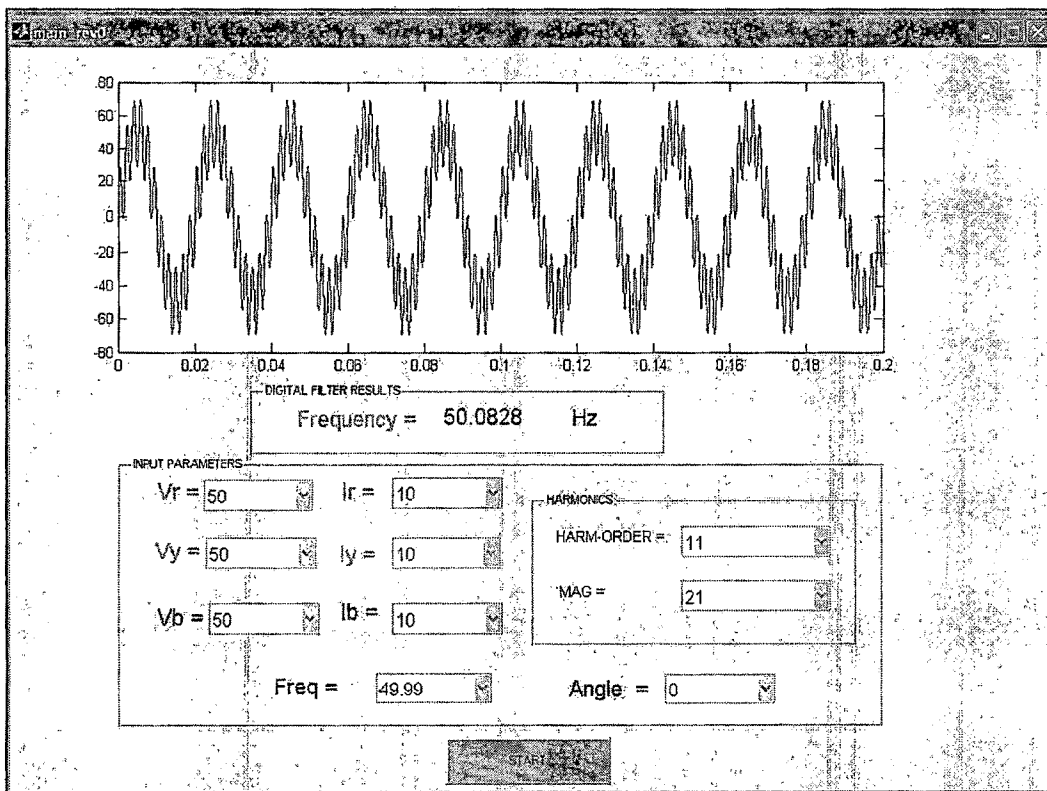


Fig. 2.7-15

Results of the freq measurement under multiple zero crossing

❖ **Case -3 Freq Measurement Under Inter-harmonic Condition**

The performance of proposed method is also tested when sub-harmonic of 1/3rd of the fundamental signal is present. Table 2.7-5 indicates the error obtained at various frequencies. Fig. 2.7-17 shows the plot of error obtained under sub-harmonic conditions.

Condition:	Sub Harmonic Conditions		
Sr.No	Actual Frequency (Hz)	Measured Frequency (Hz)	Error (%)
1	46.12	46.17	-0.10841
2	46.54	46.47	0.150408
3	47.08	47.18	-0.2124
4	48.97	48.94	0.061262
5	49.99	49.96	0.060012
6	50	50.012	-0.024
7	51.09	50.98	0.215306
8	52.29	52.34	-0.09562
9	53.01	52.97	0.075457
10	54.95	54.991	-0.07461

Table 2.7-5 Freq Measurement under sub harmonic Conditions

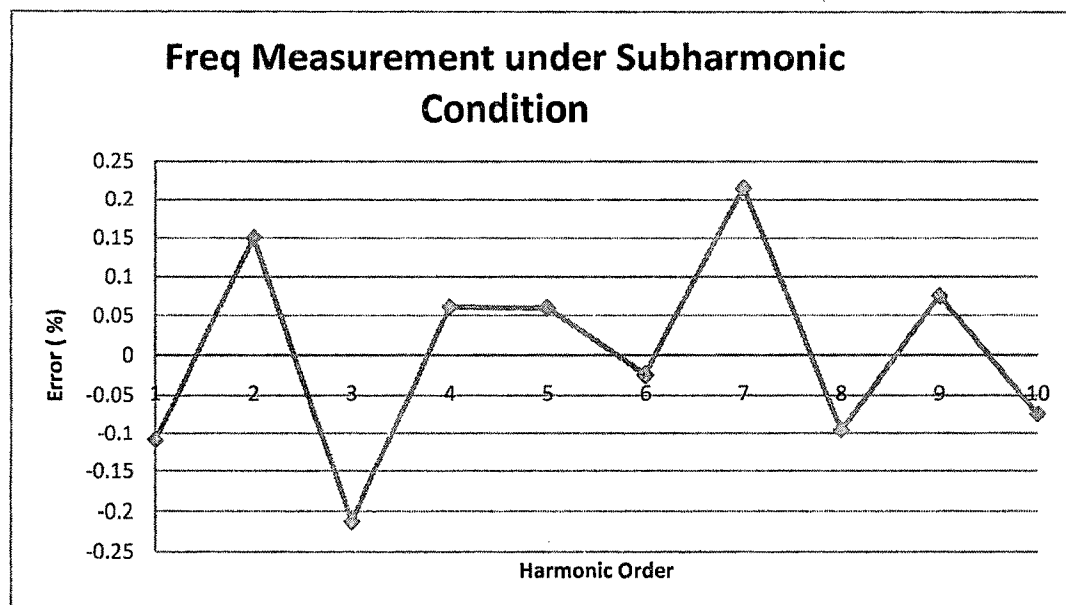


Fig. 2.7-16 Comparison results for frequency measured under sub harmonic conditions

2.8 Methodology for Frequency Measurement

Three phase voltage and current signals are stepped down to DSP by using a Potential Transformer (240/1V) and Current Transformer (5/1 Amp).

The Digital Signal Processor (DSP) used to deploy the algorithm is TMS320F2806. The DSP is 16-bit fixed point DSP with internal 12-bit Analog to Digital Converter. The ADC in the DSP is the uni-polar ADC. The bipolar signal of P.T and C.T are converted to uni-polar by using a level shifter circuit which is described detail chapter 6. The uni-polar signals (V_r , V_y , and V_b) are then given to DSP board. The DSP samples all six channels at a sampling frequency of 1000Hz, and at 200 samples per cycle. Three phase voltage is then converted into two phase signals using the instantaneous alpha-beta theory.

The reference voltage signal is calculated and instantaneous values of reference signal are given to the digital filter as described in block diagram. All digital

filters described above are implemented in the DSP by buffering the coefficients of filter in flash memory. The DSP total computational time for a single instruction is 50ns this enables to implement fast computation of frequency estimation.

The DSP calculates frequency of input signal and stores each frequency value sample by sample in circular buffer. The designed Five DSP circuit multiprocessor architectures are interconnected to each other using the SPI (Serial Peripheral Interface). As soon as the Slave DSP receive request from master, the frequency values are transferred to master. The details of the SPI interface are given in chapter 6.

2.9 Hardware and Software

The DSP card designed for frequency measurement was connected to the other cards via SPI interface. The description of the SPI and its waveforms can be found in chapter 6. Fig. 2.9-1 shows the multiprocessor system. An in house Visual Basic based Software is developed for real time monitoring of various power quality parameters. A screen shot for the frequency displayed on the computer screen is shown in the Fig. 2.9-2.

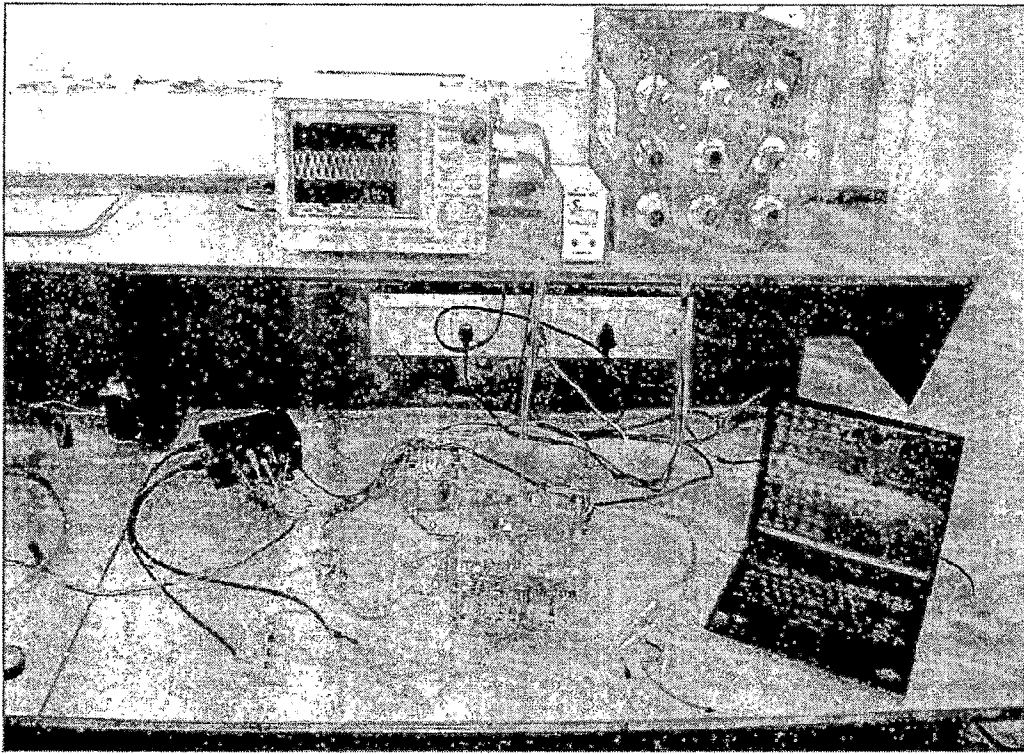


Fig. 2.9-1 Multiprocessor architecture for power quality measurement

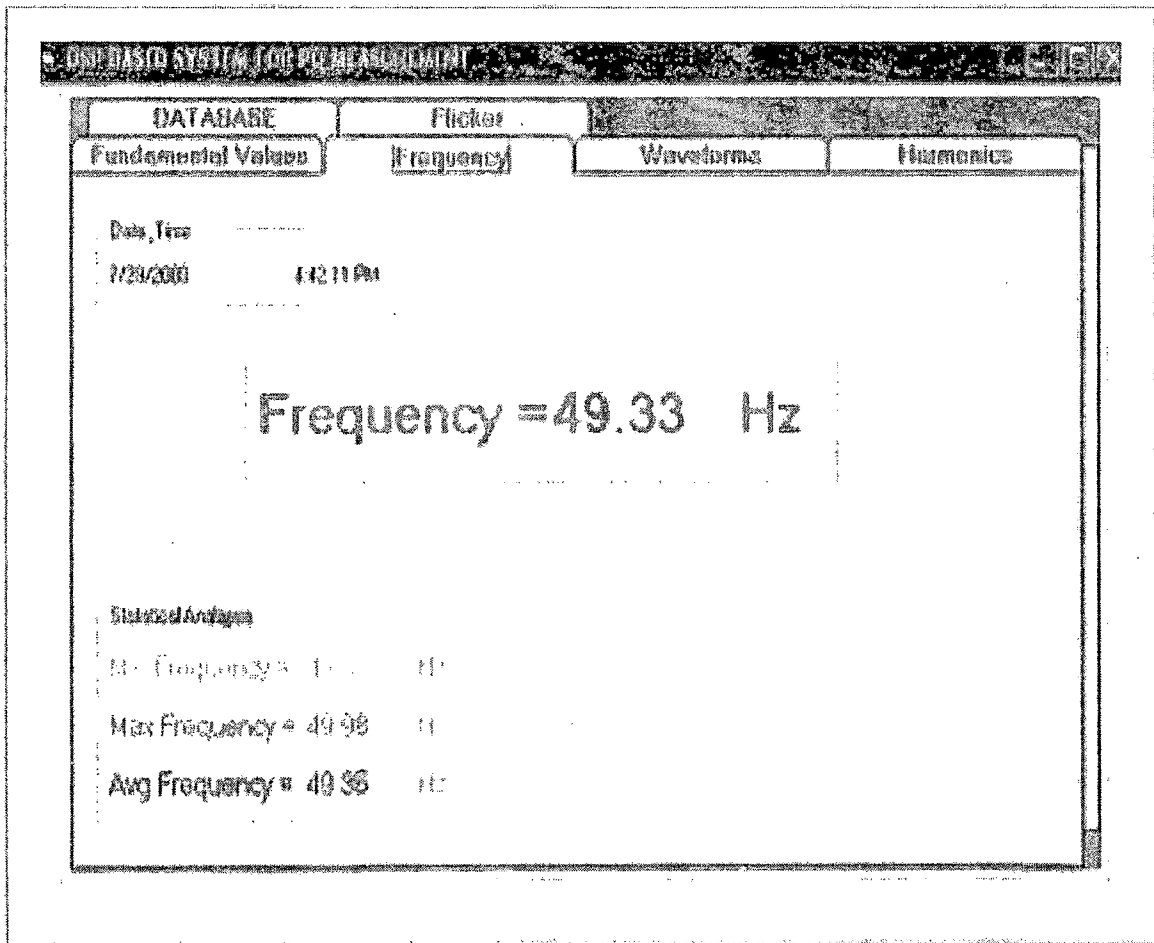
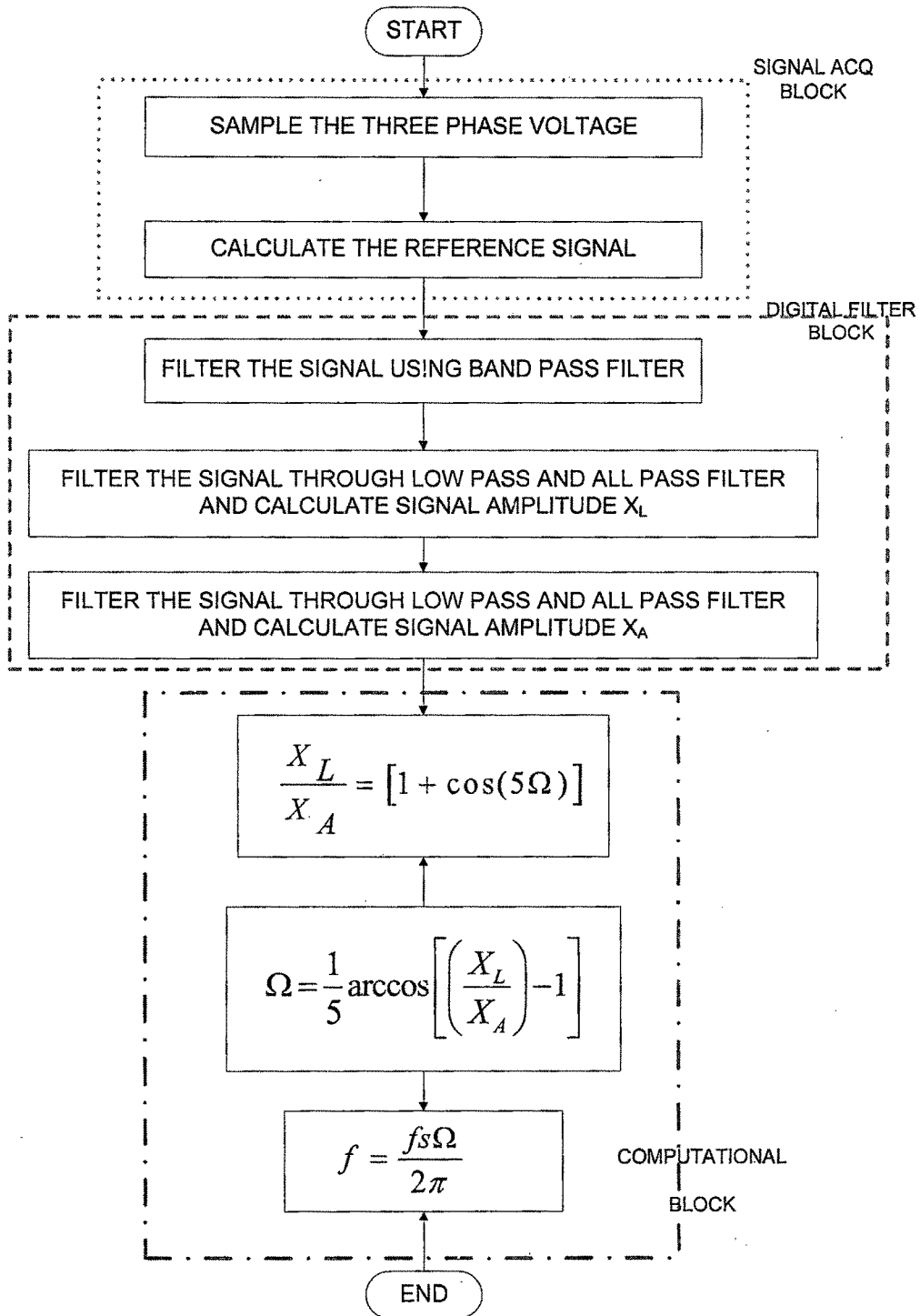


Fig. 2.9-2 Screen Shot for Frequency Measurement

2.10 Flowchart



2.11 Results

The system is tested with the available 3-phase Variac source (240Vac, 15Amp). The same was also compared with the calibrated oscilloscope. A screen shot of the frequency displayed on the computer and oscilloscope interface with the computer is shown in Fig. 2.11-1. A comparison table for the frequency measured by the hardware based on the proposed model with calibrated oscilloscopes is shown in Table 2.11-1.

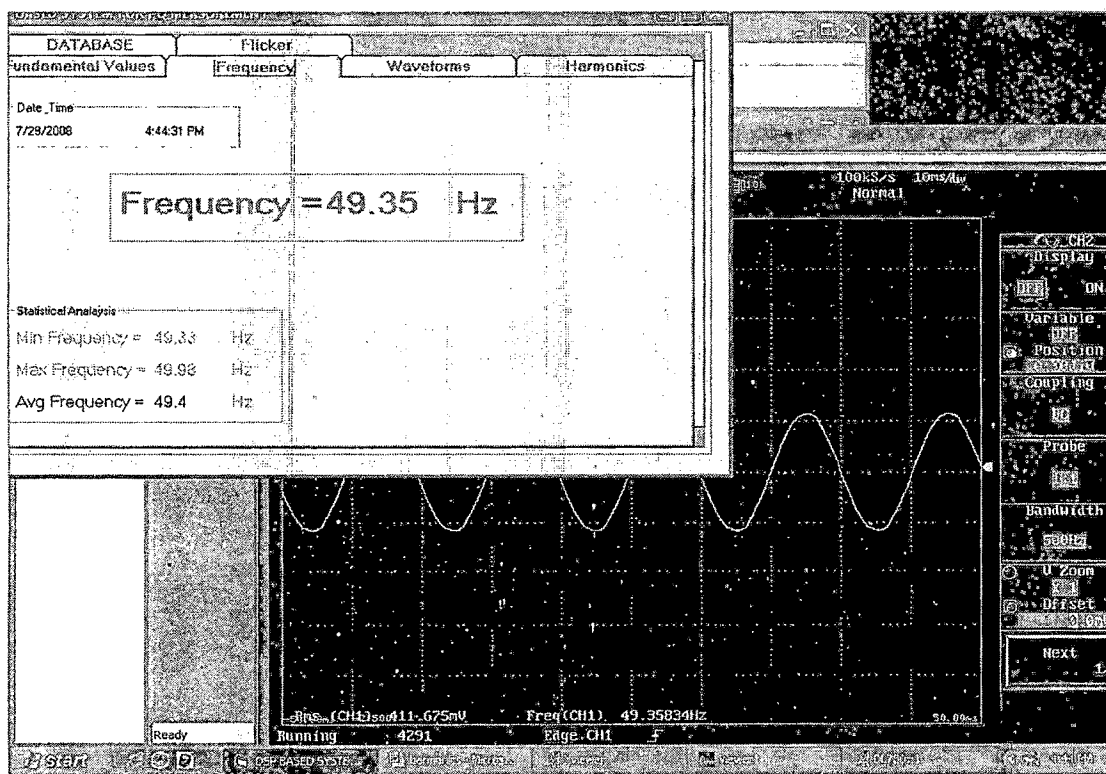


Fig. 2.11-1 Screen shot of the software and Oscilloscope interfaced to PC

Condition: Results of Actual Hardware			
Sr.No	Actual Frequency (Hz)	Measured Frequency (Hz)	Error (%)
1	49.8604	49.8599	0.001003
2	49.8629	49.8619	0.002005
3	49.8654	49.8647	0.001404
4	49.8679	49.8669	0.002005
5	49.8629	49.8624	0.001003
6	49.8729	49.8719	0.002005
7	49.9124	49.912	0.000801
8	50.1217	50.121	0.001397
9	49.8651	49.8647	0.000802
10	49.9136	49.9129	0.001402

Table 2.11-1 Comparison and Error obtained on actual hardware

2.12 Conclusions

In this chapter, algorithm for frequency measurement have been derived using digital filter (using IIR and FIR) and its performance under various abnormal conditions such as harmonics, sub-harmonics, noise and multiple zero harmonic conditions. Also a method to compute frequency sample by sample has been derived so as to compute frequency faster and accurately as compared to conventional technique. The Mathematical model has been developed for single phase and three phase condition. Error obtained under sinusoidal and non-sinusoidal has been discussed under various conditions.

The illustrative calculations carried out for different harmonic conditions confirm the validity of the proposed algorithm. Based on the computation and findings of the proposed algorithm, following conclusions have been drawn:

- Frequency measurement using zero crossing conditions works effective during sinusoidal conditions and is prone to error under multiple zero crossings, harmonics and sub-harmonic conditions. The time required to compute the frequency is more than one cycle.
- Zero crossing method is simpler to implement and can be implemented where only measurement is required and not for protection system.
- Digital filters can be effectively utilized for measurement of frequency, they can be easily implemented on hardware. The real time measurement of frequency cycle by cycle can be achieved using the model described in this chapter. Simulation and actual results confirm the validity of the same.
- Digital filter based frequency measurement shows excellent performance under sinusoidal conditions. The error obtained by the model is much lower than the conventional frequency measurement technique.
- Effect of harmonics both in terms of magnitude and the order of harmonic is negligible on the digital filter. The Band pass filter is much effective and removes the harmonics signal present in the voltage signal.
- Performance of the digital filter under sub-harmonic condition leads to an maximum error of 0.2%.
- Performance of the digital filter is excellent in multiple zero crossing and higher order harmonics.